ENEL 400

Team Seventeen – Team # 17

Final Design Specification

Wireless Tire Temperature and Pressure Monitoring System

Dylan Rae | [redacted]

Prepared for: Denis Onen

TA: King Fai Ma

April 10th, 2020

Acknowledgements

Team Seventeen would like to express gratitude to Denis Onen, as well as the ENEL 400 Lab Technicians and teaching aids for their advice and material aid on this project. Credit is also due to the Schulich Racing team and the Schulich School of Engineering Makerspace for the shop space and guidance they provided during this project.

Table of Contents

Table of Figures

Introduction

Data is an extremely valuable resource to have in the engineering design process and when evaluating technologies. The development of race cars is no different, with data being used to make vital decisions during both the design and operational phases of the vehicle. Schulich Racing is an interdisciplinary team that designs, builds, and tests a 2/3rd scale formula one car. The team competes in a SAE regulated competition against 80 other collegiate teams from around the world. To continually improve the performance of the vehicle, the team relies heavily on data to make educated decisions that will further improve vehicular performance.

The ability to operate tires in the optimal operating range is vital to achieving the full performance potential of the race car. In order to operate the tires in the optimal operating range, the team requires data about the pressure and temperature of the tires as these are significant factors affecting tire performance [1]. This data can be used during the design phase and during the operational phase for tuning the car. Additionally, the data would also be used to prevent long-lasting temperature differentials forming across the tires which can lead to premature tire wear. This uneven wear can lead to an uneven surface where only parts of the tire are able to contact the ground.

This report details the design solution created by Team Seventeen for the wireless TTPMS. The hardware block diagram and software block diagram are included demonstrating the hardware layout and software design. Each component of the block diagram is then described in detail along with a more in-depth explanation of the software operation. The engineering analysis performed, and alternative designs considered is then discussed along with a description of the enclosure and PCB design process. Finally, future work that could be performed to enhance the solution is described.

1.1 Acronyms and Abbreviations

ADC – Analog to Digital Convertor
CAN – Controller Area Network
CSA – Canadian Standards Association
DLL – Data Link Layer
FOV – Field of View
GPIO – General Purpose Input-Output
GUI – Graphical User Interface
IEC – International Electrotechnical Commission
IEEE – Institute of Electrical and Electronics Engineers
IR – Infrared Radiation
ISO – International Organization for Standardization
LED – Light-Emitting Diode
PCB – Printed Circuit Board
SAE – Society of Automotive Engineers
SD – Secure Digital
TTPMS – Tire Temperature and Pressure Monitoring System

USB – Universal Serial Bus
UML – Unified Modeling Language
USD – United States Dollar
WBS – Work Breakdown Structure

2 Predecessor Works

Currently, a comparable product exists for purchase from a company called IZZE racing. Their sensor offers up to 100Hz sampling frequency, 16 channels per sensor (for transient surface temperature analysis), and a ±1ºC temperature accuracy. This product fulfills all our design requirements; however, it is extremely expensive at a price of $1700 USD. This predecessor work provided our team with a valuable design that we could reference when developing our solution. Below in Figure 1 are images of the IZZE product:

Figure 1: IZZE Wireless Tire Temperature Sensor

In addition to the IZZE product, our team has valuable resources available with the Schulich Racing Team. The Schulich Racing Team has many members who can assist us with PCB design, sensor selection, and most importantly, mechanical design advice for our enclosure. Furthermore, the team can provide us with additional shop space and specialized equipment.

3 System Block Diagram

3.1 Hardware Block Diagram

The hardware block diagram below (Figure 2) depicts the high-level hardware design of the wireless TTPMS. The wireless TTPMS design consists of a temperature sensor module that contains three ZTP-315 IR temperature sensors, a 3:1 multiplexer, an INA325 Instrumentation Amplifier and a Wheatstone bridge. The ZTP-315 are contactless temperature sensors that each have a thermopile and a thermistor sensor. The thermopile sensor converts the infrared radiation (thermal radiation) into electrical energy, specifically an analog millivolt output. The three outputs are then fed into a 3 to 1 multiplexer (TS5A3357) controlled by the microcontroller module. The output of the multiplexer is then amplified by an INA325 Instrumentation Amplifier

to a voltage range that can be read by the microcontroller module. The other thermistor sensor produces a resistance value based on the ambient temperature. This electrical resistance value is then read by a Wheatstone bridge. The Wheatstone bridge outputs the measured voltage read across the two legs of the bridge circuit. This outputted voltage is then read by the microcontroller module.

The TTPMS design also consists of a pressure sensor module that contains a KP235 pressure sensor. This sensor detects the barometric pressure and outputs a respective analog voltage for a specific pressure to the microcontroller module. The microcontroller module consists of an ATMEGA328P chip (the chip used in an Arduino Nano) to then process the analog inputs and outputs. This microcontroller module is powered by coin cell batteries in series to generate a 6V supply. The 6V supply is regulated by a 5V regulator and a 3.3V regulator to output a constant 5V and 3.3V supply.

The TTPMS design also consists of a Transceiver Module that each contain a NRF24L01 wireless module that transmits and receives the data outputted from the microcontroller. The data is then sent to another microcontroller which then forwards the data to a Java program that converts the analog voltages into their respective temperature and pressure values. More information about the software and the software block diagram can be found below in section 3.2.

The design we choose to implement seeks to be light weight, small, low powered and modular to meet our project's design constraints and requirements. It was vital for the design to be small and light weight as many of the hardware block diagram modules shown in Figure 2 are located and operating inside of a tire. To make the design lighter and smaller, only the ATMEGA328P chip was used instead of an Arduino nano in the microcontroller module. Also, only one Wheatstone bridge was implemented as well as only one instrumentation amplifier with a multiplexer. This not only reduced space on the PCB and made the design lighter, but it also made our design lower powered. This was crucial to meet one of our constraints (constraint 4.2) that our design had to have a battery life greater than 5 hours. Our design is also modular, allowing for more and/or different sensors to be added to expand the functionality or increase the accuracy of our project, as the microcontroller module can receive input from various analog sources and output data to any user interface, SD card or database chosen.

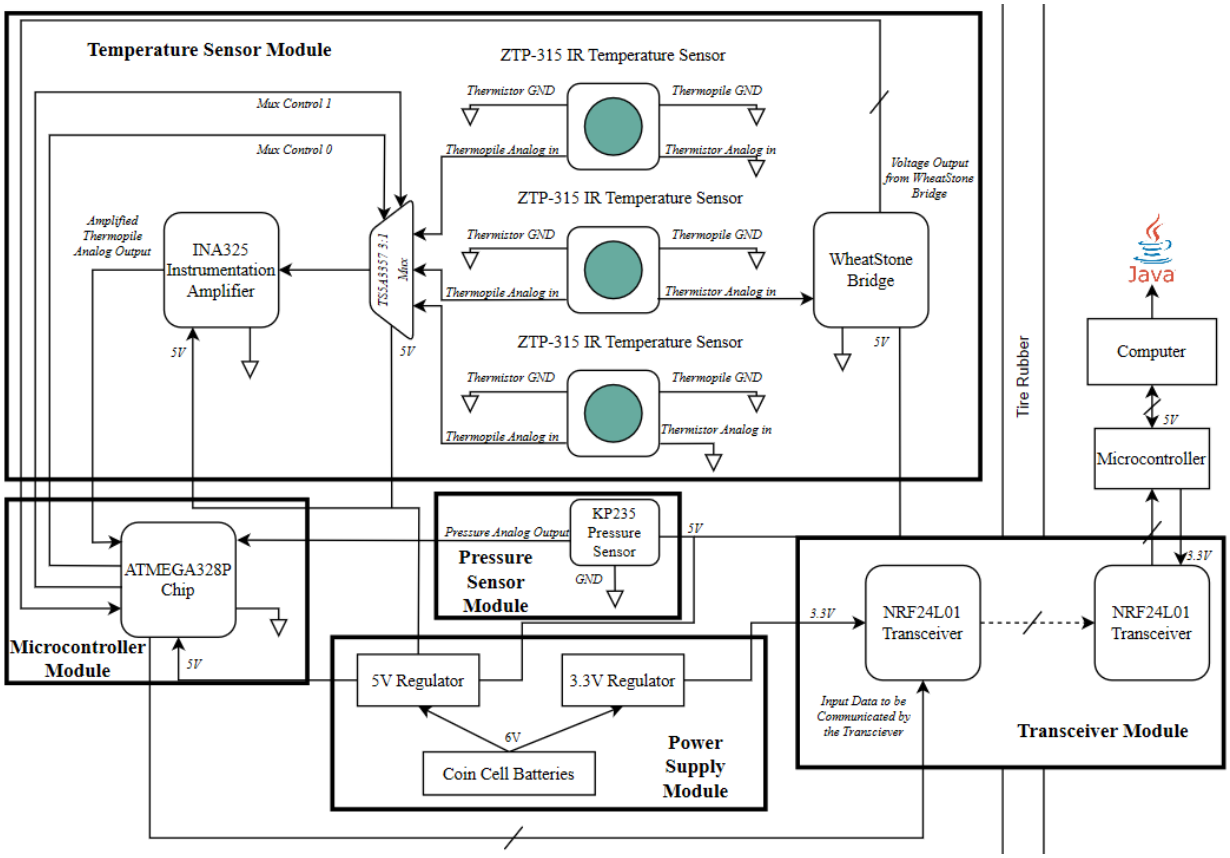

Figure 2: High Level Hardware Block Diagram (In-Tire Module)

3.2 Software Block Diagram

Figure 3 is a high-level view of how the in-tire module and base receiver firmware operate. It also displays the view of how the Java visualization software receives and processes this data. Expanded details about each block are included in Section 4.2.

Figure 3: High Level Software Block Diagram

4 Block Descriptions

4.1 Hardware Block Descriptions

4.1.1 Temperature Sensor Module

The temperature sensor module includes the temperature sensors themselves, as well as additional hardware required to prepare the temperature sensor outputs for the microprocessor. Each ZTP-315 sensor has an output for both the thermopile and thermistor. Since all three sensors are near each other, the team decided to use only one thermistor output for determining the ambient temperature of the sensors. A Wheatstone bridge is implemented for determining the resistance value of the thermistor. A Wheatstone bridge was used due to the low power consumption of the circuit, and the high degree of accuracy the bridge provides. More information on the design and analysis for determining ambient temperature is available in section 5.1.2.

Since the output of the thermopile sensors on the ZTP-315 is in the range of -4mV to 11mV, an amplifier is required to make it compatible with the 5V system operating voltage. The amplifier implemented is an INA326, a single-supply, rail-to-rail, instrumentation amplifier. More information on the amplifier design and selection is available in section 5.1.4. To reduce the power required to amplify the thermopile voltage and the spatial requirements of the design, a 3:1 TS5A3357 multiplexer is used. More information on the design of the multiplexer is available in section 5.1.5. The microprocessor selects which thermopile to read from with select lines Mux Control 1 and 0 (Figure 4) to cycle through the different sensors. The microprocessor then reads the amplified thermopile output voltage along with the Wheatstone bridge voltage to determine tire temperature. Figure 4 shows the block diagram for the temperature module, while Figure 5 shows the amplifier layout, and Figure 6 shows the layout of the 3:1 multiplexer.

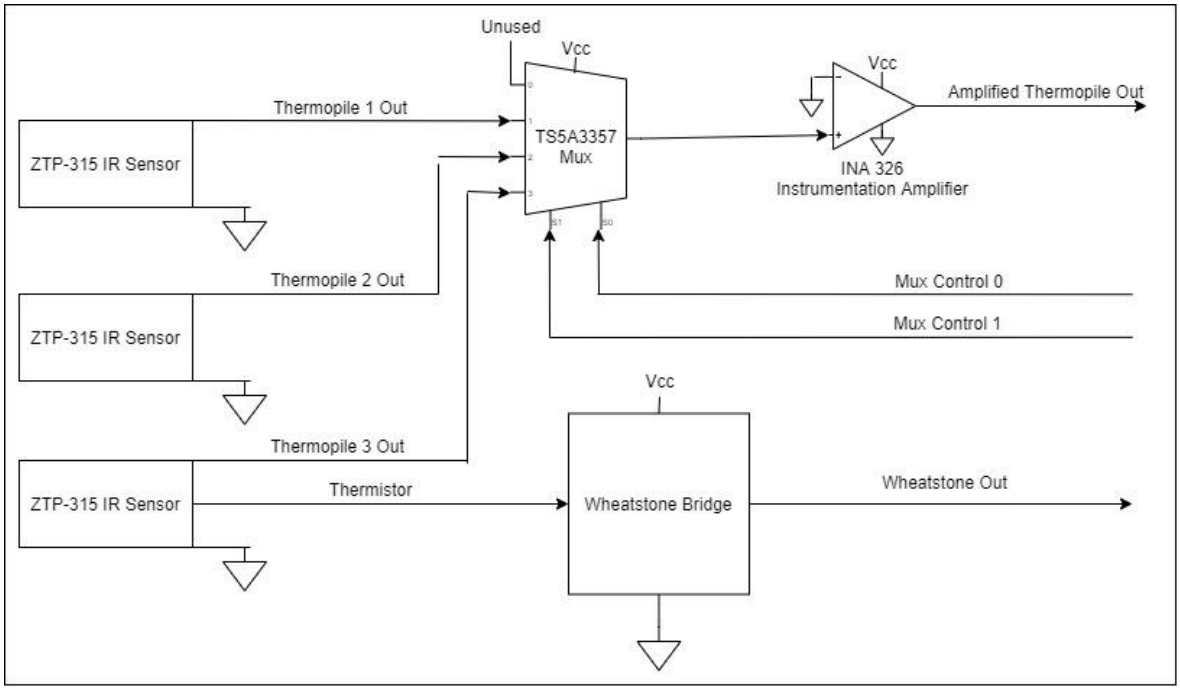

Figure 4: Temperature Module Block Diagram

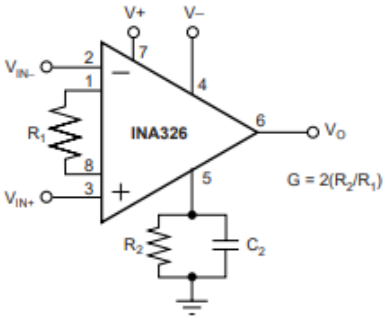

Figure 5: INA326 Instrumentation Amplifier Configuration

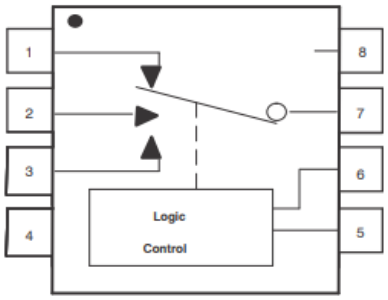

Figure 6: TS5A3357 3:1 Multiplexer

4.1.2 KP235 Pressure Sensor Module

Below is the schematic for the pressure sensor module.

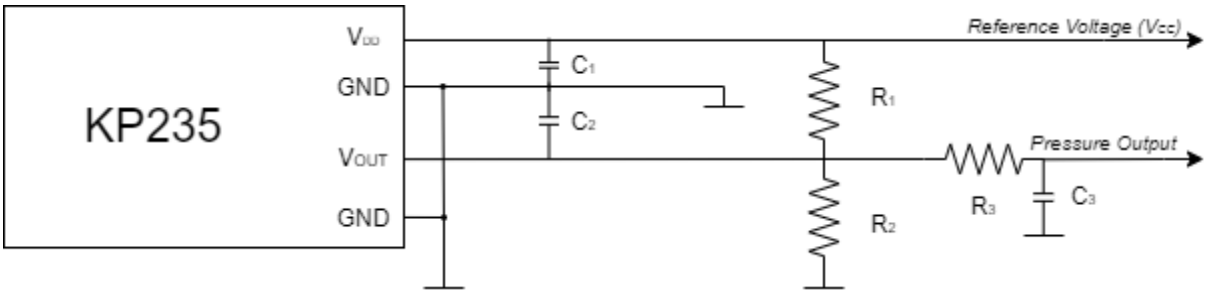

Figure 7: KP235 Pressure Sensor Schematic

For our implementation of the pressure sensor, we opted to use the recommended circuit provided by the manufacture. This was due in part to both the convenience of using their layout for design, as well as their application fit well within our own project requirements. The output circuit acts as a low pass decoupling filter between the sensor IC output and the analog/digital input of the microcontroller. This circuit protects the pressure sensor against overload and electromagnetic interferences. The values for the resistors and capacitors we used are provided in Table 4.1 below.

Table 4.1 Component Values

Component	**Symbol**	**Value**	**Unit**
Pull-up Resistor	R_1	59	kΩ
Pull-Down Resistor	R_2	59	kΩ
Low Pass Resistor	R_3	22	kΩ
Supply Blocking Capacitor	C_1	100	nF
Output Blocking Capacitor	C_2	100	nF
Low Pass Capacitor	C_3	100	nF

4.1.3 Transceiver Module

Below is the pin layout of the nRF24L01 transceiver module.

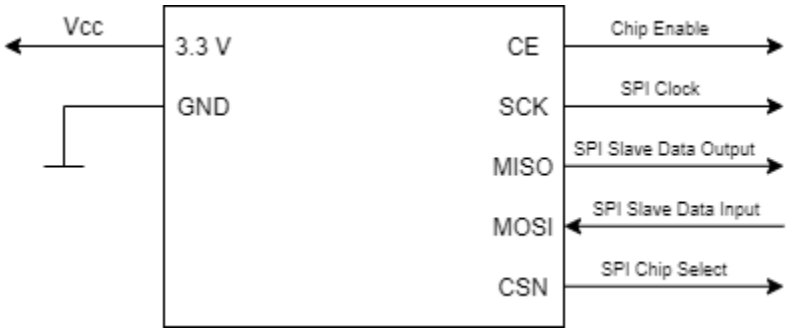

Figure 8: Transceiver Block Diagram

Since our project heavily depended on the wireless communication, we opted to use a very simple and commonly used antenna. The selected transceiver is designed to communicate over the desired 2.4 GHz band. The antenna runs at 3.3 V and is ultra-low power with a maximum current draw of 13.5 mA, whilst receiving at 2 Mbps. Finally, since the transceiver came with a communication protocol developed by Nordic Semiconductor, there was no need to develop or work with a new communication protocol.

4.1.4 Microcontroller

The microcontroller acts as a communication hub between both the sensors as well as the receiver module. The digital select pins allow the microcontroller to select which input to the mux is to be read next. The microcontroller controls which of the 3 IR sensors is being read at a given moment as well as continuously reading the pressure and ambient temperature values.

Then, in real time, the microcontroller sends the above readings to the transceiver to be sent to the central, on-board device.

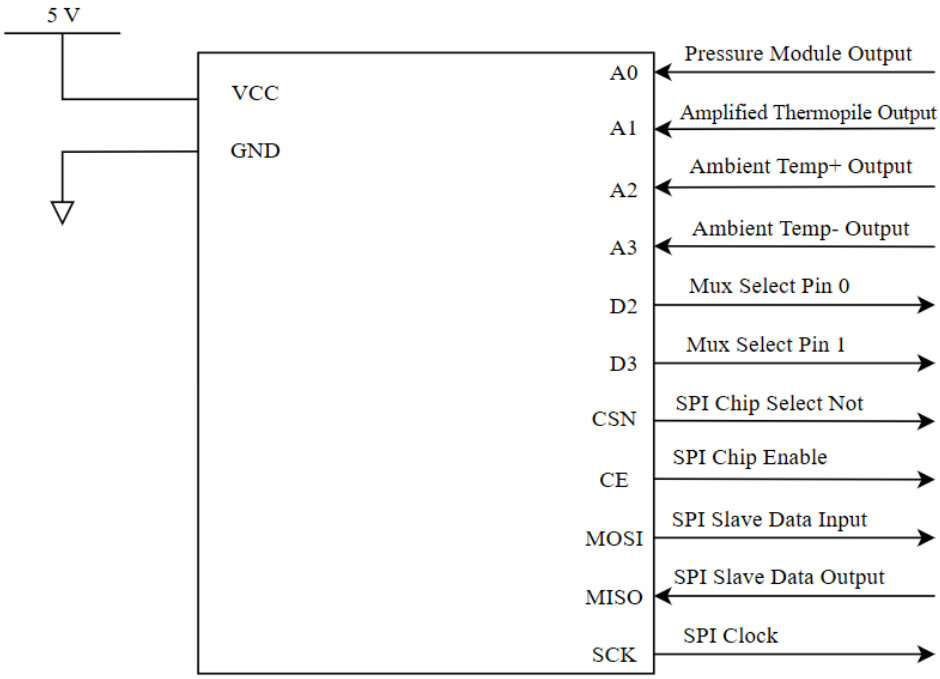

Figure 9: Microcontroller Block Diagram

4.1.5 Power Supply

As a completely independent device, the in-tire module requires its own source of power. The team decided to use coin cell batteries for this project, as they are compact and light while still being able to supply enough power to run the module. Two 3V 2032-coin cell batteries will be used in series to provide 6V source voltage. Due to the specific voltage requirements of our electrical components, the voltage will need to be brought down to the system operating voltages of 5V and 3.3V. For this purpose, two linear regulators will be used.

4.2 Software Block Description

From a high level, the software of the TTPMS can be separated into three separate blocks. These are the in-tire module, the on vehicle base receiver, and the off-site data processing system. The flow of information from the sensors begins at the in-tire module and is eventually led to data processing system where it can be translated into a human-readable form. A primary feature of our design is the ability for the singular base receiver on the vehicle to communicate with a variable number of in-tire modules. We can think of the base receiver simply as a link to collect data from the various in-tire modules and re-send such data to a central computer on the vehicle which already has the responsibility of collecting vehicle data. The off-site data processing system is an example of how the data can be reported in real time to race team members for further analysis.

4.2.1 In-Tire Module

The primary function of the in-tire module software is to collect and send the raw sensor data at the request of the on-vehicle base station. Once the radio and ADC hardware has been initialized, the in-tire microcontroller enters an infinite loop where the radio's receiver buffer, which stores any incoming messages, is constantly queried to check if a command has been sent by the base receiver. The module may receive a command to sleep, or to begin collection of the sensor data and respond back to the base receiver with packetized data. If the module is commanded to sleep, it enters a low power mode for one second before awaking and checking the radio's receiving buffer for a new command. Once a "send data" command is received, the microcontroller immediately samples the appropriate 5 ADC ports connected to the various sensors and with that constructs a packet ready for transmission. The packet, which simply organized the collected data into a known format, is placed into the radio's transmission buffer, the microcontroller switches the radio to transmission mode and the command to transmit is executed immediately. Once the microcontroller requests the radio to transmit, the module returns the radio to its receiver mode and begins waiting for a new command from the base receiver.

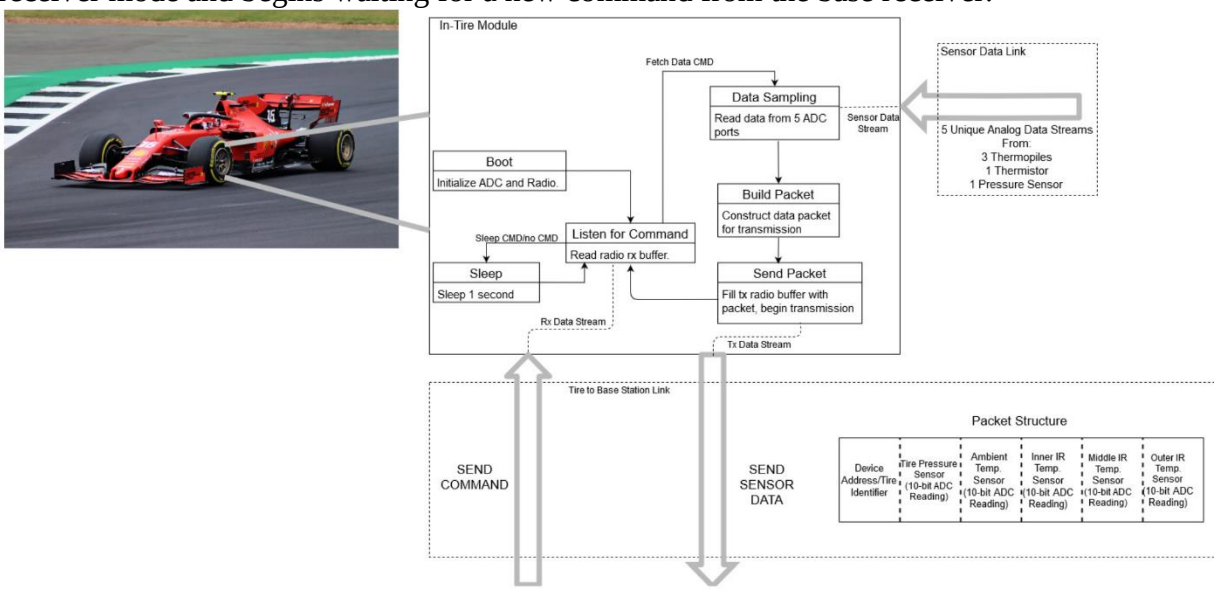

Figure 10: In-Tire Module Block Diagram

4.2.2 Base Receiver

At the heart of the TTPMS' operation is the base receiver; whose primary function is to collect data from the various in-tire modules and forward that data to an off-vehicle data processing system. During typical race operation, the base receiver boots up and initializes its radio, and proceeds to send a one-byte beacon or command to all the in-tire modules requesting data at a rate of 20Hz. However, as access to the in-tire modules is physically challenging and impractical, the base receiver also has the option of sending all in-tire modules to sleep to save power by sending a "sleep" command. The operation to send a "sleep" command is triggered by a button on the microcontroller. Once a "send data" command has been sent, the base receiver switches its radio's operation to receiver mode and enters a loop to continuously checks the

radio's receiving buffer for any incoming messages. Once a message is received, the packet of data is logged on an on-board SD card. The message is also forwarded to a central data collecting computer that collects all vehicle sensor data before returning its radio to its transmission mode and sending another command to all in-tire modules. The specifics of the link between the central computer and the base receiver remains ambiguous as the objective of the TTPMS was to construct a tire data collection framework which could be implemented in a variety existing system rather than be tailored to a specific one. The specifics of this communication link are not extremely relevant in the operation of the software, but for our own testing we connected the base station to a laptop through USB and serialized the data before sending it to be processed on the laptop.

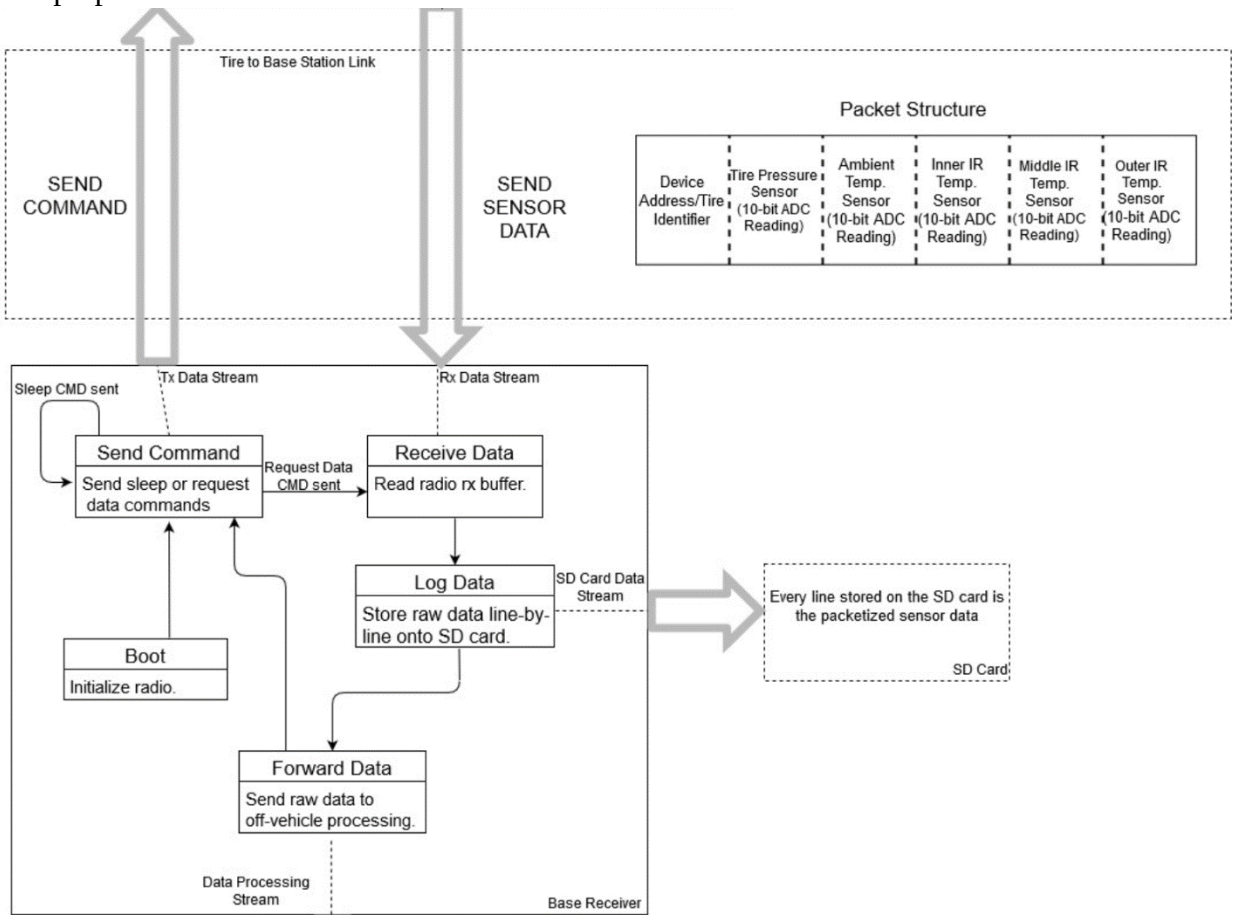

Figure 11: Base Receiver Block Diagram

4.2.3 Data Processing/Visualization

In order to be able to use the live data while the car is in use, there must be a process in place to get that data to the driver or the rest of the team. We have created a software package written in Java that can read the data from the base station through a serial link. The package uses the JSerialComm library [1] to receive sensor data from the base station, and the Java Swing library to display the live data and to visualize the current state of the tire's surface temperature. The software reads the incoming messages from the serial port connected to the receiving transceiver. This transceiver sends the incoming data in a string format that can be easily converted by the Java program. The software then converts the voltage readings to the corresponding temperature and pressure values. A high-level view of the operation of this visualization software can be seen in the software system block diagram (Figure 3) as well as in Figure 12 below.

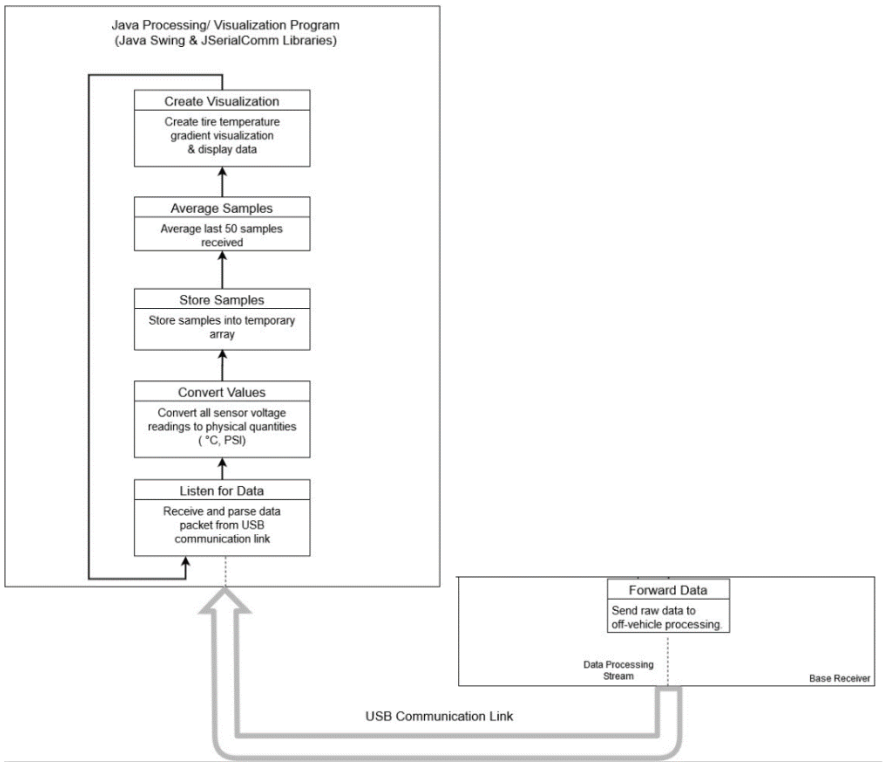

Figure 12: Graphical User Interface (GUI) Block Diagram

The window displayed by the software shows the absolute pressure inside the tire, as well as the surface temperature of the tire on the outer edge, inner edge, and in the middle. To easily interpret the surface temperature data, a color gradient is shown. The gradient goes from blue to green to red. A blue location corresponds to a cold surface temperature on the tire, and a red location corresponds to a hot surface temperature on the tire. Two samples of the software are shown in Figure 13.

Figure 13: Two Sample Outputs from GUI

Note: Due to the COVID-19 situation, development on this software was halted, and the software is restricted to functioning with a single tire. Expanded functionality for receiving data from multiple tires was planned but was not executed.

5 Engineering Analysis

5.1 Temperature Sensor Module

5.1.1 ZTP-315 IR Temperature Sensor Operation and Calibration

The team selected the analog ZTP-315 thermopile IR sensor to act as the temperature sensor for our solution. The sensor uses several thermocouples connected to series to form the thermopile. The thermocouples operate by producing a voltage when a temperature differential across the device is created. The thermopile in the ZTP-315 is designed to produce a voltage across its terminals by detecting an objects IR. IR is generated by thermal radiation, which is a type of electromagnetic radiation generated by particles of matter. The ZTP-315 detects IR in the ranges of 3-5µm and 8-12µm wavelengths which are common ranges for thermal radiation emitted by everyday objects. Using Plank's law of black-body radiation, the temperature of the object emitting the thermal radiation can be calculated where B_v is the spectral radiance, h is the Plank's constant, c is the speed of light, k is the Boltzmann constant, v is the frequency of the electromagnetic radiation and T is the absolute temperature of the object.

$$B_v = \frac{2hv^3}{c^2}\frac{1}{e^{\frac{hv}{kT}} - 1}$$

Equation 1: Plank's Law of Black-Body Radiation

The manufacturer of the ZTP-315, Amphenol Advanced Sensors, provides the following equation for estimating a given objects absolute temperature, assuming the object is a black-body. This equation is derived from Plank's law, Stefan-Boltzmann's law, and the Seebeck

effect. Our research shows that tire rubber is a close approximation for a black body (95%) [2] meaning the below equation can be used to calculate an objects temperature.

$$output\ voltage = S({T_o}^{\beta} - {T_A}^{\beta})$$

Equation 2: Thermometrics Thermopile Equation

Where S is the sensitivity coefficient (determined by measurement), T_o is the objects temperature, T_A is the ambient temperature, and β is 4 (sensor construction). Ambient temperature is required because the output voltage from the sensors thermopiles is highly dependent on ambient temperature. Since the team did not get the opportunity to calibrate the ZTP-315, we used data provided by the manufacturer to estimate our sensitivity coefficient.

Figure 14, as seen below, shows the thermopile output voltage for varying object temperature in ºC at a constant ambient temperature of 25 ºC. Using a plot digitizer, data points were extracted from this plot for further analysis. Since this graph provides us with output voltage, T_o, and T_A, we can solve for S, the sensitivity coefficient using equation 2. By analyzing the error between the mathematically predicted output and the plot, a sensitivity coefficient can be selected to minimize this error. Figure 15 shows an error analysis for varying values of the sensitivity coefficient. After consultations with the Schulich Racing Team, it was determined that precision was preferred over accuracy of the sensor. As such, the sensitivity coefficient with the lowest standard deviation was selected because on average this sensitivity coefficient will predict values closest to the plot's values.

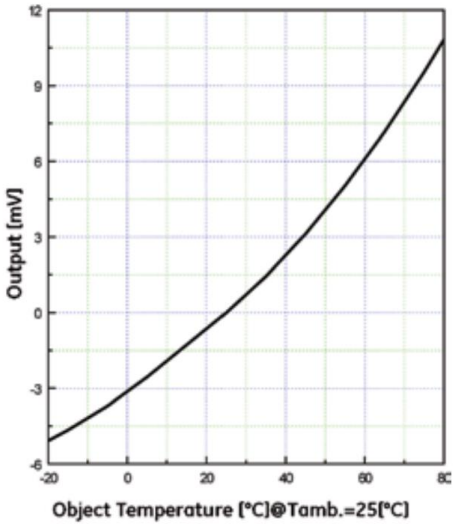

Figure 14: Thermometrics ZTP-315 Output Voltage versus Object Temperature

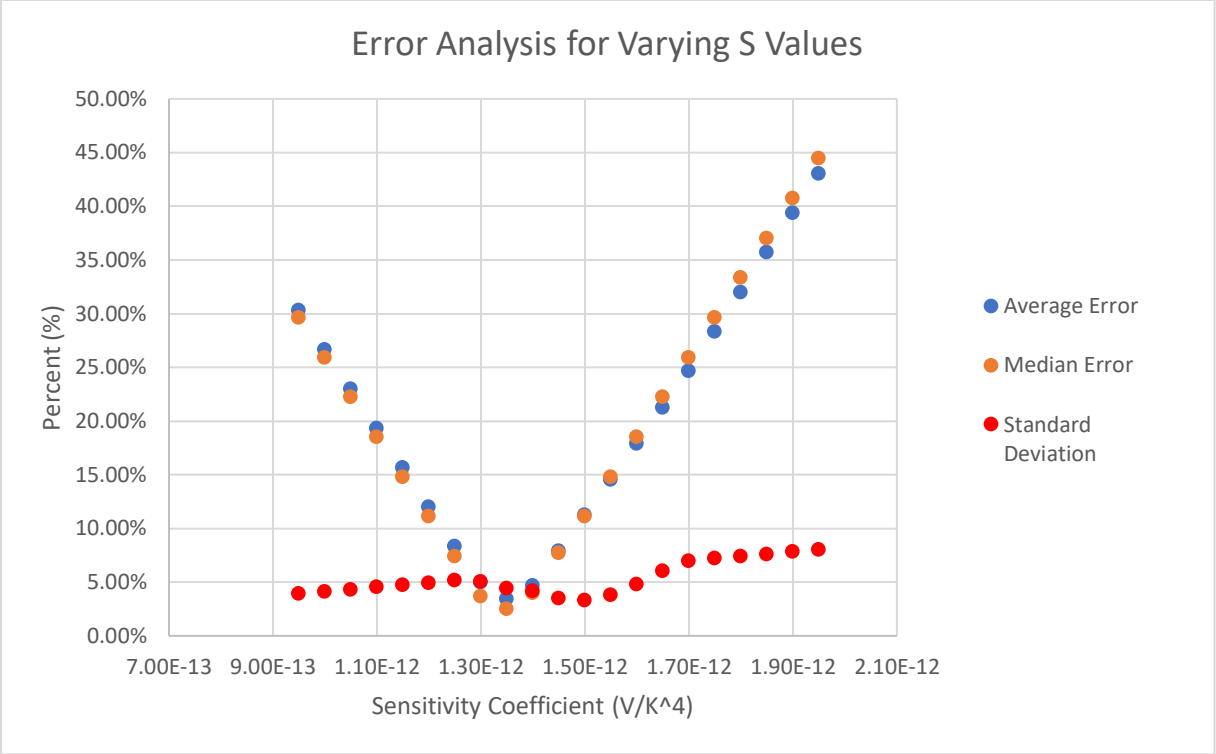

Figure 15: Error Analysis for Varying Sensitivity Coefficient Values

This specific model (ZTP-315) was chosen for a variety of reasons. First, the sensor offers a wide FOV which can be easily adjusted with filtering to suit our needs. Second, the sensor is passive and does not include any other components such as an on-board amplifier. This allowed us to have a custom amplification circuit that minimizes power consumption and has amplification properties the team designed for. Additionally, the stand-alone sensor makes it easy to minimize spatial requirements as we only need to include components necessary for our solution. Next, the ZTP-315 has a high sensitivity and fast response making it possible for the team to make accurate temperature measurements and have a very high sampling frequency if desired. Finally, the ZTP-315 is low-cost ($7.50 each) and easy to source as it is widely available from electronic part suppliers.

5.1.2 Ambient Temperature Circuit Design

Given that the temperature sensor module is going to be in a harsh environment with widely fluctuating ambient temperatures, our solution uses the thermistor built into the ZTP-315 to calculate the ambient temperature. The manufacturer provided data table an equation relating thermistor resistance to ambient temperature is as follows:

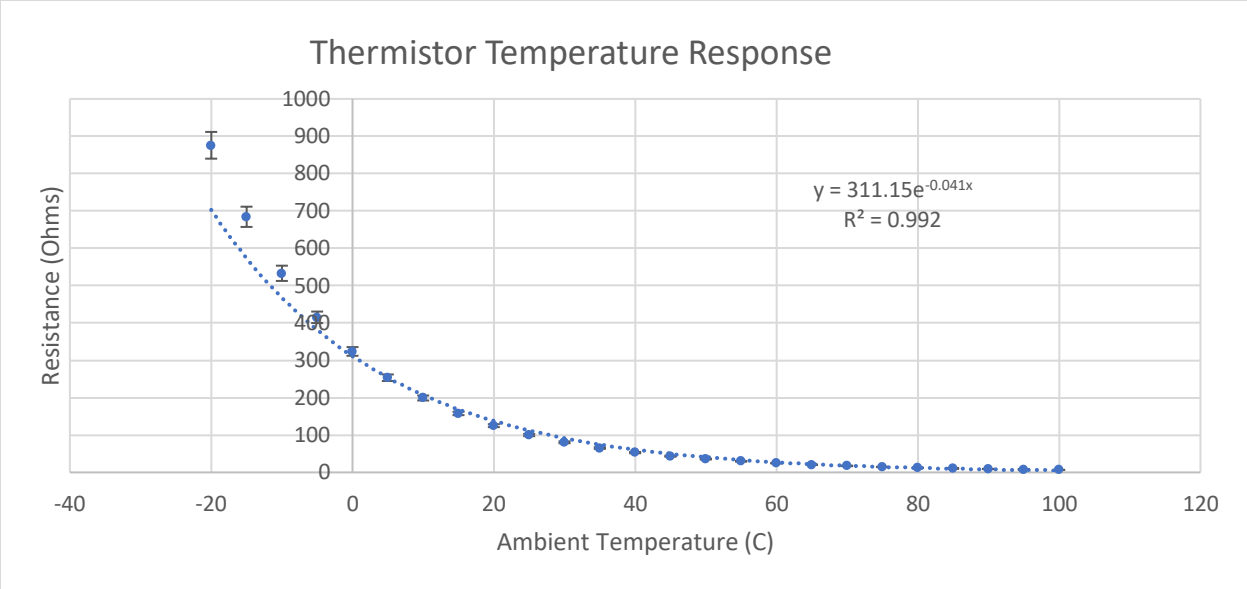

Figure 16: Plot of Thermistor Resistance as a Function of Temperature

$$Resistance = 311.15e^{-0.041 * ambient\ temperature}$$

Equation 3: Relationship Between ZTP-315 Ambient Temperature and Thermistor Resistance

To measure the resistance of the thermistor, a Wheatstone bridge and voltage divider circuits were designed and analyzed.

The Wheatstone bridge uses a connection of 3 fixed resistors, and one resistor of unknown resistance. In our case, the thermistor is the unknown value $\mathbf{R_x}$. The voltage output of the thermistor, $\mathbf{V_g}$, is proportional to the resistance of the thermistor. To optimize for minimal current draw, and maximum precision, different resistance values were chosen, and the current draw and precision were calculated. Precision was quantified by taking the difference between the voltage reading at minimum temperature (0ºC), and maximum temperature (100ºC). A larger absolute 'spread' between these two values would allow for greater precision when measuring $\mathbf{V_g}$. From the table below, a preliminary analysis (with the three fixed resistor values being equal) determined the best resistor value to use is 500,000Ω. With 500,000Ω resistors, current draw is minimized (table 5.1).

Similar analysis was done with a simple voltage divider circuit. The optimized circuit resulted in similar voltage spread, but a higher current draw (see table 5.2 for details). Therefore, the Wheatstone bridge design was selected to measure ambient temperature.

Table 5.1: Wheatstone Bridge Preliminary Analysis

R1, R2, R3	V_g @ 0 C Ambient	V_g @ 100 C Ambient	Voltage Spread	Maximum Current Draw (µA)
500	4.98	4.24	0.741	5756.43
1000	4.97	3.59	1.376	3203.23
2000	4.94	2.53	2.405	1866.52
5000	4.85	0.50	4.348	950.05
10000	4.70	-1.21	5.908	560.37
20000	4.42	-2.66	7.078	316.50
40000	3.90	-3.67	7.575	170.94
50000	3.66	-3.91	7.573	139.11
100000	2.64	-4.42	7.065	72.12
200000	1.18	-4.70	5.885	36.76
300000	0.19	-4.80	4.991	24.67
400000	-0.53	-4.85	4.323	18.56
500000	-1.07	-4.88	3.810	14.88
600000	-1.49	-4.90	3.404	12.42
700000	-1.84	-4.91	3.076	10.65

System Values	
V_{system}	5 V
R_x @ 0 C	3.238E+05
R_x @ 100 C	6.110E+03

$$V_G = \left(\frac{R_2}{R_1 + R_2} - \frac{R_x}{R_x + R_3} \right) V_s$$

$$R_x = \frac{R_2 \cdot V_s - (R_1 + R_2) \cdot V_G}{R_1 \cdot V_s + (R_1 + R_2) \cdot V_G} R_3$$

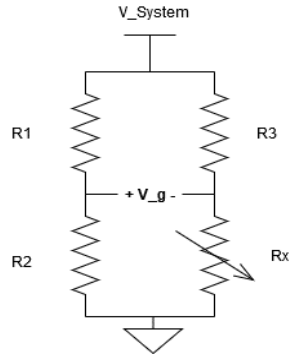

Table 5.2: Voltage Divider Analysis

$R_{balance}$	V_{out} @ 0 C Ambient	V_{out} @ 100 C Ambient	Voltage Spread	Maximum Current Draw (µA)
500	0.01	0.38	0.37	57.22
1000	0.02	0.70	0.69	98.91
2000	0.03	1.23	1.20	152.04
5000	0.08	2.25	2.17	202.54
7500	0.11	2.76	2.64	202.45
10000	0.15	3.10	2.95	192.65
20000	0.29	3.83	3.54	146.69
30000	0.42	4.15	3.73	115.04
40000	0.55	4.34	3.79	94.07
50000	0.67	4.46	3.79	79.41
70000	0.89	4.60	3.71	60.42
100000	1.18	4.71	3.53	44.41

System Values	
V_{system}	5 V
$R_{thermistor}$ @ 0 C	3.238E+05
$R_{thermistor}$ @ 100 C	6.110E+03

$$R_{thermistor} = \left(\frac{V_{System}}{V_{out}} - 1 \right) R_{Balance}$$

$$V_{out} = \frac{V_{system}}{\frac{R_{thermistor}}{R_{balance}} + 1}$$

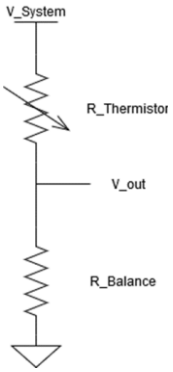

5.1.3 Temperature Sensor Shielding

Due to the wide field of view (FOV) of the ZTP-315 thermopile sensors (70-80 degrees), the sensors would likely have overlapping detection areas on the tires. To ensure each sensor is detecting a unique part of the tire, it was necessary to restrict the FOV of each sensor using the opening surrounding the ZTP-315 on the enclosure. To help with designing this opening, a testing apparatus in Figure 17 was designed in SolidWorks to gather data about how depth and angle of the opening affected the FOV of the sensor. Along the x-axis of the device, the angle of the opening for each sensor increases, while along the y-axis the depth of each opening increases.

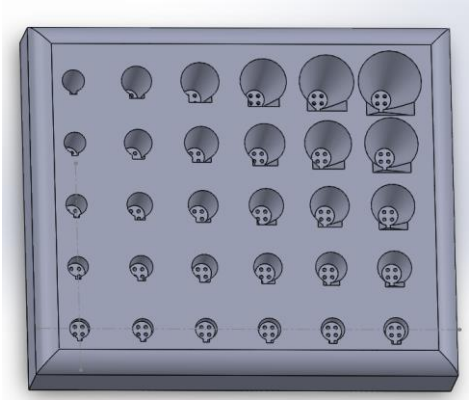

Figure 17: Temperature Sensor FOV Testing Apparatus

While the team did not get the opportunity to conduct testing with this apparatus, the testing plan was to make measurements of the devices FOV at each testing point on the device. Using this data, an equation relating FOV to depth and opening angle could be developed. This equation would be used to give us the depth and opening angle for the temperature's sensor opening when being installed on various tire sizes and mounting positions.

5.1.4 INA326 Instrumentation Amplifier

Since the ZTP-315 is a passive sensor with an output range of -4mV to 11mV, an amplifier is required to amplify the output signal to work with the 5.5V operating voltage of the design. The INA326 manufactured by Texas Instruments was selected to amplify the ZTP-315 thermopile output voltage. The INA326 is a precision rail-to-rail instrumentation amplifier that uses true single-supply operation. An instrumentation amplifier was selected due to the very low DC offset, low drift, low noise, very high open-loop gain, very high CMMR, and very high input impedance as these are all very important metrics for amplifying a signal with characteristics such as the thermopile output voltage. The overall gain of the amplifier is described by the equation:

$$G = 2\frac{R_2}{R_1}$$

Equation 4: Gain for INA 326 Instrumentation Amplifier

The location of R_1 and R_2 can be seen in Figure 5 in section 4.1.1. Since the ADC on the microprocessor will have an operating voltage of 5V, we set the gain such that highest temperature the TTPMS will be required to measure will be amplified to 5V. This is done so that we can utilize the maximum range of the ADC and thus have the highest degree of accuracy in our thermopile output voltage readings. Since the highest tire temperature we are interested in measuring is 80ºC, we set the gain so that the voltage corresponding to this temperature is amplified to 5V. 80ºC has a corresponding thermopile output of 11mV at an ambient temperature of 25ºC. These values were obtained from Figure 14. To find the gain required, we divide 5V by 11mV to get a desired gain of 455. To set R_1 and R_2 manufacturer recommendations were followed. The manufacturer of the INA326 recommends the optimum value for R_1 by following the below equation:

$$R_1 = \frac{V_{IN_{MAX}}}{12.5\mu A}$$

Equation 5: Optimum Value for R_1 in INA326 Instrumentation Amplifier

Following this equation, we get a R_1 of 880Ω. However, R_1 must not be less than 2kΩ according to manufacturer specifications. Using the new R_1 value of 2kΩ, R_2 is calculated to be 455kΩ using equation 4. While the team did not get the opportunity to test this amplifier, further testing was planned to obtain the optimal gain for the solution.

5.1.5 TS5A3357 3:1 Multiplexer

The TS5A3357 3:1 multiplexer is used to reduce the power required to amplify the thermopile signal before being read by the microcontroller. The datasheet for the INA326 states current draw will be 2.4mA. Figure 18 shows the current draw for the proposed multiplexer, drawing approximately .492mA at our estimated operating temperature. By implementing the multiplexer, we reduced the current draw of 3 amplifiers (7.2mA) by 60% to 2.892mA by using just one amplifier connected to a multiplexer.

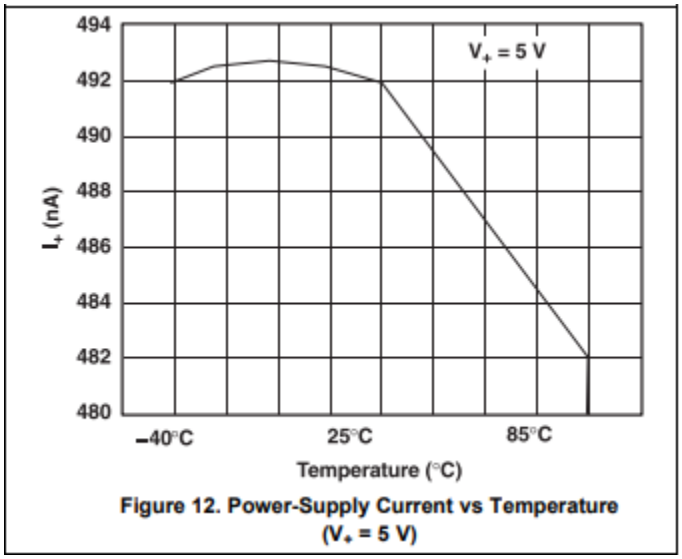

Figure 18: TS5A3357 3:1 Multiplexer Current Draw

This specific model of multiplexer was chosen due to several features that make it effective for our application. First, the packaging is very desirable, with a chip size of 2.3mm x 2mm. Next, the device offers low ON-state resistance and low input-output capacitance resulting in minimal signal distortion. To further reduce signal distortion, this multiplexer features break-before-make switching allowing clean transfer of a signal from one port to another. This means that introducing a multiplexer will have very low impact on both spatial requirements and signal quality. The time to switch between inputs (Break-before-make time t_{BBM}) is 0.5ns which is fast enough to support a sampling frequency much higher than our requirements. Additionally, the TS5A3357 is low-cost ($0.95) and is widely available from electronic parts suppliers.

5.2 Power Supply Module

Two regulators are required to convert from the 6V supply voltages to the system operating voltages. Linear regulators were chosen because of their stability, reliability, and small area requirements. A switching regulator was considered because of its efficiency; however, it would require more space for its complex PCB layout requirements and the complexity could introduce more sources of error to our project. A high confidence in the product working correctly is required for this project, and a compact solution is ideal, so it was decided that a switching regulator was not the correct decision for this project. The increased efficiency of the switching regulator was also found to not be required due to the batteries chosen for the project and the current requirements for the components. 2032-coin cell batteries have a capacity of approximately 240 mAh. The approximate current requirements for the major components of the project are as follows:

Table 5.3: Summary of Expected Current Draw for Major Electrical Components

Atmega328P Microcontroller	13 mA
NRF24L01+ Transceiver	12 mA
KP235 Pressure Sensor	1.0 mA
INA326 Amplifier	2.4 mA
TS5A3357 Multiplexer	.492 mA

Doing a simple calculation with these values, it can be found that, using linear regulators:

$$Battery\ Life = \frac{240}{13 + 12 + 1 + 2.4 + 0.492} = 8.31\ hours$$

This significantly exceeds the project requirement for a battery life of 5 hours, so linear regulators are found to have enough efficiency for the project. Two 3V 2032-coin cell batteries will be used in series to provide a source voltage of 6V, and then two linear regulators will be used to achieve the required operating voltages: 3.3V for the transceiver, and 5V for everything else.

5.3 Data Storage

As an added redundancy to the TTPMS, collected data in the base receiver block is stored on an on-board SD card to ensure any data loss further down the system is accounted for. The data being stored on the SD card would be an exact copy of our transmitted packet stored as a plaintext file. As determined in section 5.4.1, the maximum size of our data packet would not exceed 70 bits at a maximum. In our proposed use case scenario, the transmission rate of an in-tire module would be at most 20Hz. As a result, if four in-tire modules were all collecting and sending data consecutively, the maximum about of data we would need to store locally would be 70bits * 20Hz * 4 modules = 5600b/s or 700B/s. The time it would take to fill a 1GB SD card would be 10GB / 700B/s = 1428571s or 396 hours of continuous data logging. Therefore, using a 1GB SD card would be no issue.

5.4 Transceiver

5.4.1 Determining Bitrate Expectations

According to the datasheet of the NRF24 radio module, the lowest possible transmission data rate is capped at 250kbps, for when the link budget is maximized. In the most unoptimized configuration for our packet structure, where we would send all information as a string of characters, the size of the packet would not exceed 70 bits. Additional information such as CRC bits, preamble header, and packet control which is combined with our payload packet within our chosen firmware library would bring the total size of our transmission to 103 bits (refer to NRF24 datasheet). If we attempt to transmit messages at 20Hz, the resulting throughput would be slightly above 2kbps, leaving us well within our data rate budget.

Table 5.4.1: Data value sizes for the required transmitted data types

Data	Device Address	Thermopile Reading	Thermistor Reading	Pressure Reading
Maximum value	N/A	2^{10}	2^{10}	2^{10}
Maximum size (bits)	40	10	10	10

Note: Maximum value of readings for sensor values is derived from the resolution of the microcontroller's ADC. The maximum value of the device address is given in the NRF24 datasheet as 5 bytes.

5.4.2 Frequency Band Selection

The initial step in deciding which transmitter to employ is to determine the most appropriate frequency band to use in transmission. Readily available for unlicensed use are the ISM bands in the 900MHz and 2.4GHz ranges. These ISM bands do not require a licensed operator for commercial deployment and as a result are very quick to implement in a product. As a result, there is a greater selection of off the shelf components which operate in the above ranges, resulting in decreased costs and greater customization for your application. The main differences

in the two proposed bands relate to the data rates and link budgets/effective transmission ranges, where the lower frequencies can achieve long range transmission at the cost of lower data rates. For our proposed use case, the required transmission range would be 1-2m, thus a 2.4GHz transmitter which are known to reliably transmit from 10-100m [3] would more than adequately meet our needs. The data rate of a typical 2.4GHz transmitter, as mentioned in section 5.4.1, would also exceed our needs, and allow for increased amounts of data transferring capabilities should a future iteration require it.

5.4.3 Additional NRF24 Radio Justification

In addition to meeting our data rate and link budget needs, the NRF24 enabled modules are designed to enable extremely low idling power. As installing the TTPMS in-tire module requires access to the inside of the race tire, ensuring that the device can consume limited power when not in use is paramount. With a power down draw of 900nA [4], the NRF24 is designed for this purpose in mind.

Furthermore, many radio modules which use the NRF24 have been designed for hobbyist use in mind, and as result, there exist many firmware libraries for use with common microcontrollers such as the Arduino family. This is especially useful in the TTPMS as it allows the team to spend more time creating more reliable and accurate measurement circuitry.

6 Enclosure

The Tire Temperature and Pressure Monitoring System is to be fitted on to the exterior of the rim of each tire on the race car. Therefore, some of our goals in making the enclosure were

- Limit the size of the enclosure
- Make the enclosure as lightweight as possible
- Have the enclosure be temperature resistant
- Have all the components securely fit, as the tire would be in constant rotation.

Our first enclosure design was introduced in our Design Review was simply to show the general idea of how it was to be fitted to the rim of the tire.

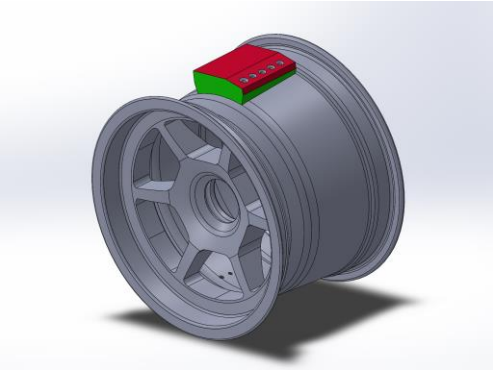

Figure 19: Initial Enclosure Design

Another consideration we had was the shielding effect on the temperature sensors. This phenomenon describes the relationship between the field of view (measured in degrees) and the proportion of the output voltage. To test this, a 3D model testing apparatus was designed and printed to help determine the dimensions of the openings for the temperature sensors. More detail on the testing apparatus can be found in section 5.1.3.

The MVP demonstration included a third enclosure design, a boxed fit which had two separate components, a bottom and a top. This piece was designed to fit the wireless transceiver, the circuit board, and the temperature and pressure sensors.

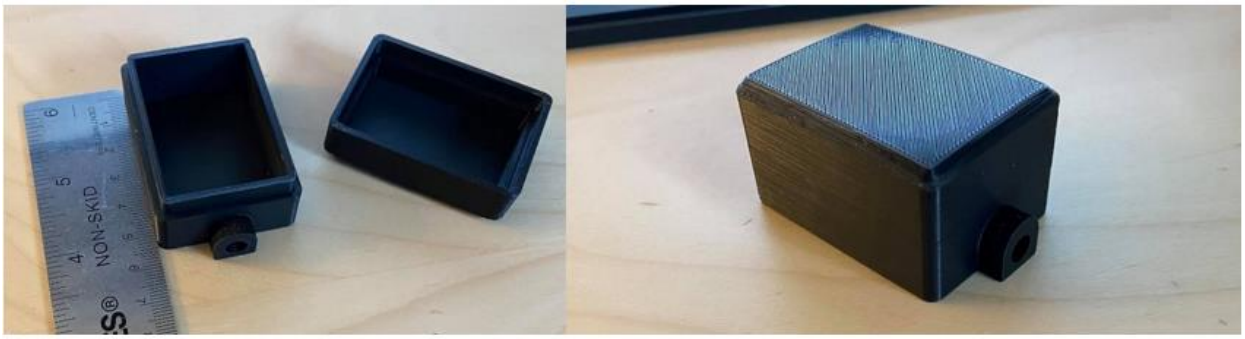

Figure 20: Enclosure Iteration for MVP Testing

This box was designed in SolidWorks and was printed in the University of Calgary Makerspace using PLA material. As shown in the left picture, it has a length of approximately 5 cm, with a width of 3.6 cm.

The final enclosure was to be a combination of the three previous iterations, taking the enclosure from Figure 20, and adding the correct temperature sensor fitting found in Figure 17. The final enclosure was to be printed in Onyx filament (mix of nylon and carbon fiber) as well, as it can keep its structural integrity at high temperatures and has great strength and durability. Onyx filament can maintain its structural integrity at higher temperatures over PLA material. This is because it has a heat deflection temperature (the temperature before material starts to deform) of 145°C while PLA material has a heat deflection temperature of 55°C [5]. Onyx is one of the few 3D printed thermoplastics that is strong enough to be used commercially [6]. This is a vital component for our final enclosure as it would meet the design's requirements of keeping the in-tire module secure and protected at higher temperatures.

7 Printed Circuit Boards

The PCB design for this project consisted of two iterations: initial prototype PCBs for the MVP presentation, and a final system PCB incorporating all in-tire electrical components. Due to COVID-19, we were not able to complete the manufacturing of the final system PCB and therefore plan to manufacture and assemble it once the University workspaces re-open.
Our team has experience with Altium Designer and has obtained use of Altium licences through sponsorship of Schulich Racing, so Altium was used for all PCB design for this project.

7.1 Prototype PCBs

The prototype PCBs were ordered through JLCPCB on February 25 and arrived March 4, giving us time to assemble and test them before the MVP demo on March 9. The cost for the PCBs was $5.52/board and the shipping was $27.45 for DHL. To save costs, we combined orders with another ENEL 400 group and split the shipping cost, bringing the total cost of obtaining PCBs for our group (without components) to $22.60. Both of our prototype PCBs worked as intended with no issues.

7.1.1 Pressure Sensor PCB

The pressure sensor chosen for this project was only available as a SMD; therefore, it was necessary to design a PCB to allow for testing of the sensor. The recommended circuit from the manufacturer was implemented for this PCB, making design quite simple. This board has 2 layers with dimensions 28x9mm. The schematic, layout, and BOM for this PCB can be found in the Appendix Sections 12.1.1, 12.2.1, and 12.3.1 respectively.

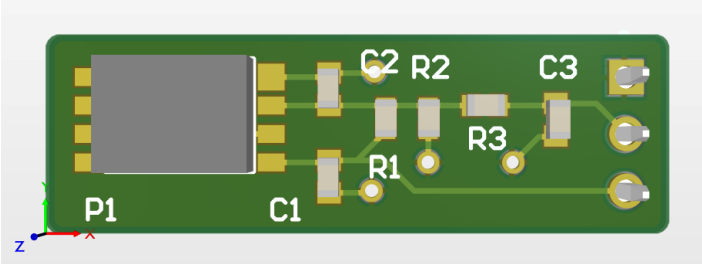

Figure 21: Altium 3D Model of Pressure Sensor PCB

7.1.2 Arduino Nano / NRF24L01+ Shield PCB

Due to the high number of connections required to connect the NRF24L01+ transceiver to the Arduino Nano we were using for prototyping, it was determined that using a breadboard would be too cumbersome and introduce sources of error that would be inconvenient when testing other areas of our system. Therefore, we designed a PCB to easily connect the Arduino Nano to the transceiver while maintaining easy access to the required analog ports on the Arduino Nano. The PCB maintained the shape of the Arduino Nano, allowing the Nano to plug in on one side and the NRF24L01+ transceiver to plug in on the other side. This PCB was only designed to make connections between the two development boards and therefore has no required components or BOM. This board has 2 layers with dimensions 43x23mm. Schematics and layout for this PCB can be found in the Appendix Sections 12.1.2 and 12.2.2 respectively.

7.2 Final System PCB

One of the main driving factors for the final PCB design was to make the sensor/transmitter end of the system as compact and efficient as possible. The end goal for this PCB design is to have all electrical components except for the NRF24L01+ transmitter on a single PCB which will have a convenient port for the transmitter to plug into. The transmitting features were not included on our PCB due to the sensitive nature of the antenna and the potential sources of error

in replicating it. The PCB will contain the pressure sensor and have mounting points for the three temperature sensors to plug into. The NRF24L01+ transmitter will connect to the back side of the PCB.
This board has 2 layers with dimensions 40x70mm. Schematics, layout, and BOM for this PCB can be found in the Appendix Sections 12.1.3, 12.2.3, and 12.3.2 respectively.

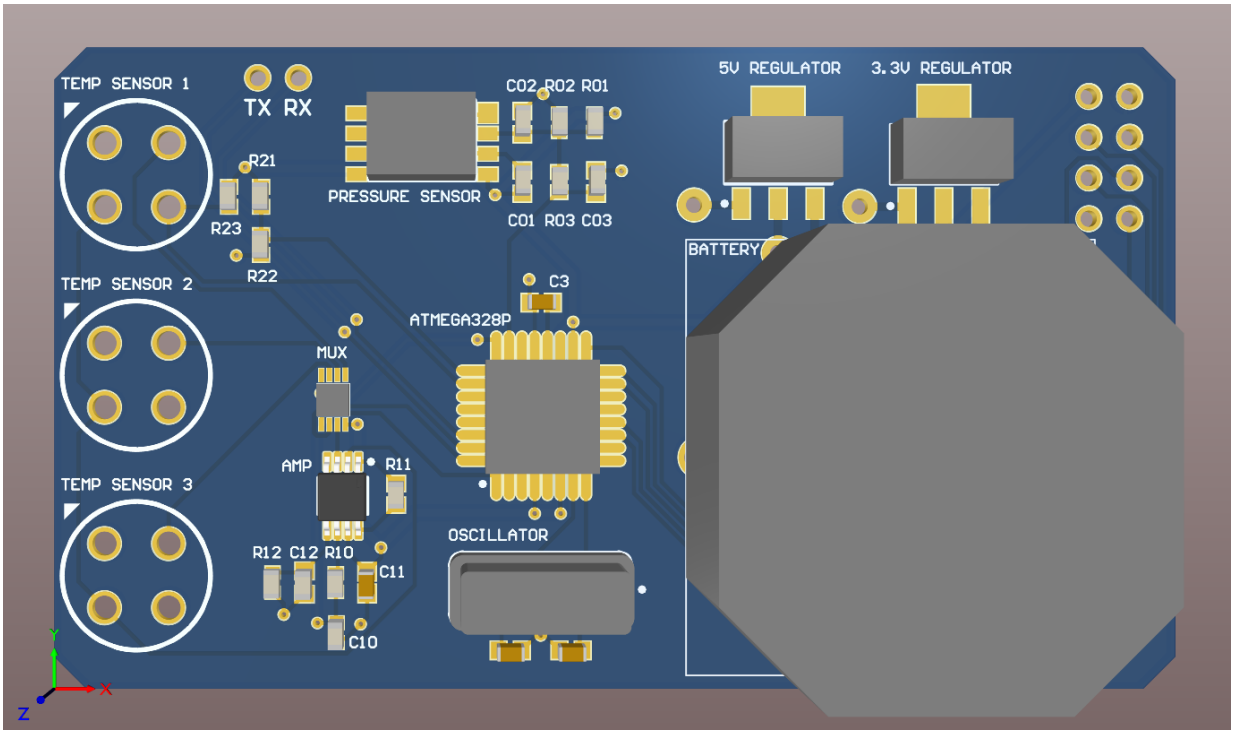

Figure 22: Altium 3D Model of Final System PCB

8 Regulatory Codes

Below are the following certifications our product would require to be taken to market.

1.1. International Organization for Standardization (ISO)
   1.1.1. ISO 9000 - Quality management to ensure that the product is of appropriate quality to meet consumers' needs.
   1.1.2. ISO-11898-1 – Specifies the DLL and physical signaling of the CAN serial communication protocol that supports distributed real-time control and multiplexing for use within road vehicles. [7]
1.2. International Electrotechnical Commission (IEC)
   1.2.1. IP66 - Provides protection against dust and other particulates, including a vacuum seal, tested against continuous airflow. Protection against direct high-pressure jets. [8]
1.3. Canadian Standards Association (CSA)

1.3.1. CSA North America Group Certification – In an umbrella context, it covers Industry Canada, FCC, and EU certification processes.

1.4. Federal Communications Commission (FCC)

1.4.1. 47 C.F.R. § 2.106 Defines the allocation of radio frequencies for specific purposes. A radio using the 2.4GHz frequency band is classified as being in the industrial, scientific, or medical devices category and the radio operator does not require any licensing to operate on that band. [9]

1.4.2. 47 C.F.R § 15 Outlines the regulations associated with the use of unlicensed transmissions. Topics such as avoiding interferences, power limitations and appropriate band usage are mentioned. [10]

To obtain these ratings, our team would work with the above organizations to complete the required tests to ensure our product meets the necessary requirements.

9 Design Alternatives Considered

9.1 Temperature Sensor Alternatives

An alternate temperature sensor considered was a digital temperature sensor (MLX90614 Digital IR Sensor) rather than the analog sensor that was chosen. Digital temperature sensors have many advantages. The largest benefit that a digital sensor provides is the ability to bypass calibration of an ADC, as one is included in the module. This reduces the hardware complexity as there is no need for using an amplifier with a calibrated gain and offset. Ultimately, we didn't choose a digital sensor due to their high cost. The MLX90614 sensor costs $57.26,and each tire in our design would require 3 sensors. A design requirement for our project was to have a cost less than $300, therefore we ended up choosing the inexpensive analog temperature sensor.

9.2 Operational Amplifier Alternatives

Before finalizing our design with the INA326 operational amplifier, several other choices were considered. The first was the LMP741, an op amp which was very accessible from the ENG 130 lab room. Through testing our team was able to determine significant factors in determining what properties were needed for an amplifier moving forward. One of these factors was the need for an amplifier that could function on single supply. This led us to purchasing the INA126 Instrumentation Amplifier. This amplifier seemed adequate for our purposes (driving a very small current from the temperature sensors), however, after countless tests we were unable to correctly configure the amplifier to function on single supply.

9.3 Communication System Alternatives

Initially, we had two hardware candidates for wireless transmission. The two options that were considered were the Nordic Semiconductor nRF52840 Dongle, and an ATmega328p (Arduino Nano) paired with a Nordic nRF24L01+ transceiver module. Initially, the nRF52840 Dongle was a very attractive solution, as it is low cost (~$10 USD each), has a small footprint, has a low power consumption and it has both a microprocessor and transceiver included in the system [11]. However, there were some limiting factors associated with using the nRF52840. Upon review of

the user guide and datasheets [12], we found that this product is not meant for development. Unfortunately, it is only for deployment of finished products that have been tested on Nordic Semiconductor development kits. We did not have the budget and resources to purchase multiple dongles, along with 2 development kits to develop and test our solution. Furthermore, the nRF52840 Dongle only has three inputs that have access to analog-to-digital converters, which is insufficient for our design. Our design requires at least 4 inputs with access to analog-to-digital converters (1 for measuring tire pressure, 2 for measuring ambient temperature from the Wheatstone bridge and 1 for measuring surface temperature from the thermopiles).

These limitations with the nRF52840 dongle, caused our group to choose the ATmega328p chip paired with a Nordic nRF24L01+ transceiver module (see Figure 24). The ATmega328p chip has enough analog input pins with access to analog-to-digital converters, as well as it has a user-friendly development environment. Furthermore, the nRF24L01+ transceiver module has Arduino compatible libraries that allow for seamless wireless communication between modules [13].

10 Future Work

To further improve our design that will be used by the Schulich Racing Team, there are several areas that could benefit from further development. The following paragraphs details the modifications and enhancements that could be done on the current iteration of our design.

One aspect of our design that could be changed and improved upon would be the microcontroller used. Currently, the system uses the ATmega328p microcontroller. This microcontroller was initially chosen as the team members had prior experience with model and support was widely available online. However, the microcontroller could be improved in two main ways. First, by choosing a microcontroller with an integrated transceiver we could greatly reduce the spatial requirements and mass of the enclosure by reducing the size of PCB. Additionally, an integrated transceiver would be more reliable by reducing risk of communication errors between the transceiver and microcontroller. Secondly, the microcontroller could be improved by selecting a microcontroller with a lower current supply requirement. Currently the transceiver and microcontroller draw a relatively large amount of current, and a more efficient hardware setup would greatly improve the battery life of the design.

The battery-life of the in-tire module is extremely important because of the way it is installed into the tire. The in-tire module is installed onto the rim, after this the tire is mounted and then balanced. This is a time-consuming and tedious process that would have to be completed every time the battery dies. To further improve battery life, a microcontroller could be selected that offers a stand-by mode. This mode would be turned on whenever the in-tire module is not being used. In this state the device would simply listen for a command to be turned back on to drastically save on power consumption. Another way to reduce power usage, would be to use a different communication protocol and band. Currently, our transceiver uses the ISM band with a simple protocol, however a different band or protocol such as ANT+ could introduce further power savings.

To improve the temperature sensor of our design, our solution could be advanced by adding additional temperature sensors to the design. The predecessor that our product is based on has 16 different channels for temperature sensing coming from one sensor, whereas our product only has 3. To reduce the size of our design and to improve the number of temperature readings, a different model of IR temperature sensors would need to be selected.

Further work that was never addressed by our team was a suitable way to attach the in-tire module to the rim. Epoxy was discussed as an adhesive to attach the module, but further testing would need to be performed to confirm that epoxy would work.

11 References

[1] Fazecast Inc., "GitHub," Fazecast Inc., 5 April 2020. [Online]. Available: https://fazecast.github.io/jSerialComm/. [Accessed 5 April 2020].

[2] I. Mikron Instrument Company, "Table of Emissivity of Various Surfaces," 03 08 2014. [Online]. Available: http://www-eng.lbl.gov/~dw/projects/DW4229_LHC_detector_analysis/calculations/emissivity2.pdf. [Accessed 2 04 2020].

[3] L. Frenzel, "The Fundamentals Of Short-Range Wireless Technology," Electronic Design, 11 October 2012. [Online]. Available: https://www.electronicdesign.com/technologies/communications/article/21798230/the-fundamentals-of-shortrange-wireless-technology. [Accessed 10 April 2020].

[4] Nordic Semiconductor, " PRODUCT SPECIFICATION," Nordic Semiconductor, [Online]. Available: https://www.sparkfun.com/datasheets/Components/nRF24L01_prelim_prod_spec_1_2.pdf . [Accessed 10 April 2020].

[5] Markforged, "Onyx Filament," 2019. [Online]. Available: https://markforged.com/materials/onyx/. [Accessed 8 April 2020].

[6] N. Martin, "PLA vs ABS vs Nylon," 19 December 2018. [Online]. Available: https://markforged.com/blog/pla-abs-nylon/. [Accessed 8 April 2020].

[7] International Organization for Standardization , "Road vehicles — Controller area network," International Organization for Standardization , 5 May 2006. [Online]. Available: http://read.pudn.com/downloads209/ebook/986064/ISO%2011898/ISO%2011898-1.pdf . [Accessed 10 April 2020].

[8] The Enclosure Company, "IP Rated Enclosures Explained," The Enclosure Company, [Online]. Available: https://www.enclosurecompany.com/ip-ratings-explained.php. [Accessed 10 April 2020].

[9] Office of the Federal Register (OFR), "Electronic Code of Federal Regulations," Government Publishing Office, 9 April 2020. [Online]. Available: https://www.ecfr.gov/cgi-bin/text-idx?SID=8f682158e27cd6f7bb3d4952e4cc35e6&mc=true&tpl=/ecfrbrowse/Title47/47cfr2_main_02.tpl. [Accessed 10 April 2020].

[10] Office of the Federal Register (OFR), "Federal Regulations - RADIO FREQUENCY DEVICES," Government Publishing Office, 9 April 2020. [Online]. Available: https://www.ecfr.gov/cgi-bin/text-idx?SID=2f25d0dbf0904584b7d3aa2223ed4741&mc=true&node=pt47.1.15&rgn=div5. [Accessed 10 April 2020].

[11] Nordic Semiconductors, "nRF52840 Dongle," [Online]. Available: https://www.nordicsemi.com/Software-and-tools/Development-Kits/nRF52840-Dongle. [Accessed 08 April 2020].

[12] N. Semiconductors, "nRF52840 DonglePCA10059 v1.0.0 User Guide v1.1," [Online]. Available: https://infocenter.nordicsemi.com/pdf/nRF52840_Dongle_User_Guide_v1.1.pdf. [Accessed 8 April 2020].

[13] tmrh20, "Optimized High Speed Driver for nRF24L01(+) 2.4GHz Wireless Transceiver," [Online]. Available: http://tmrh20.github.io/RF24/. [Accessed 9 April 2020].

[14] H. O. M. G. a. G. M. M. Furlan, "Effects of Different Tire Operating Conditions on Transient Lateral Tire Response," *Tire Science and Technology,* 2019.

12 Appendices

12.1 Appendix 1: Schematic Diagrams

12.1.1 Pressure Sensor Prototype PCB Schematic

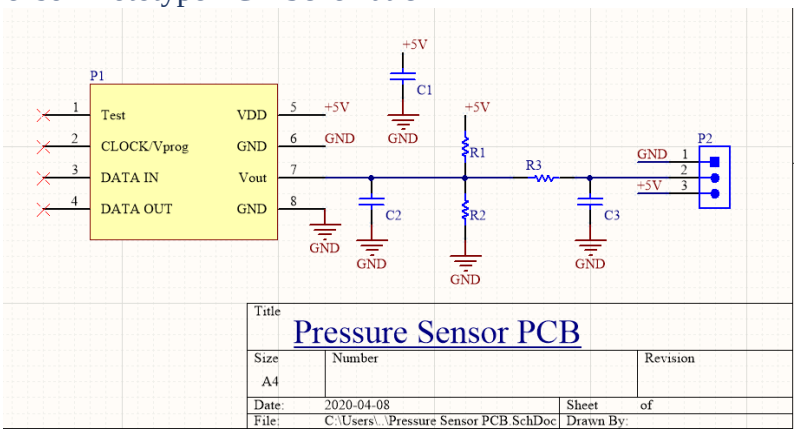

Figure 23: Schematic for Pressure Sensor PCB

12.1.2 Arduino Nano / NRF24L01+ Shield PCB Schematic

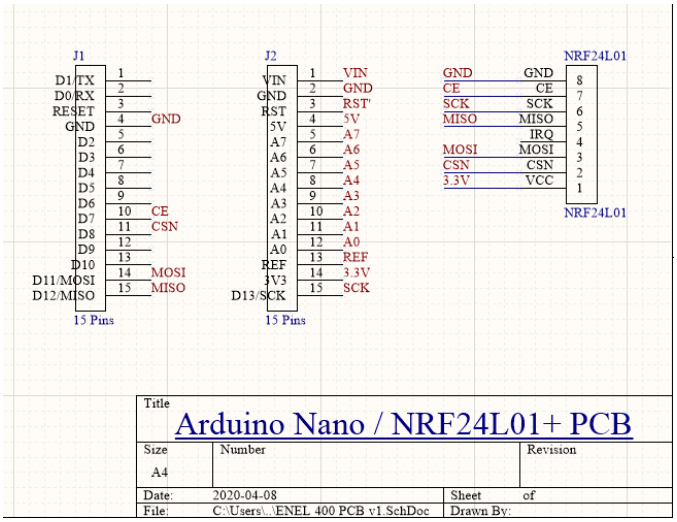

Figure 24: Schematic for Arduino Nano / NRF24L01+ Shield PCB

12.1.3 Final System PCB Schematics

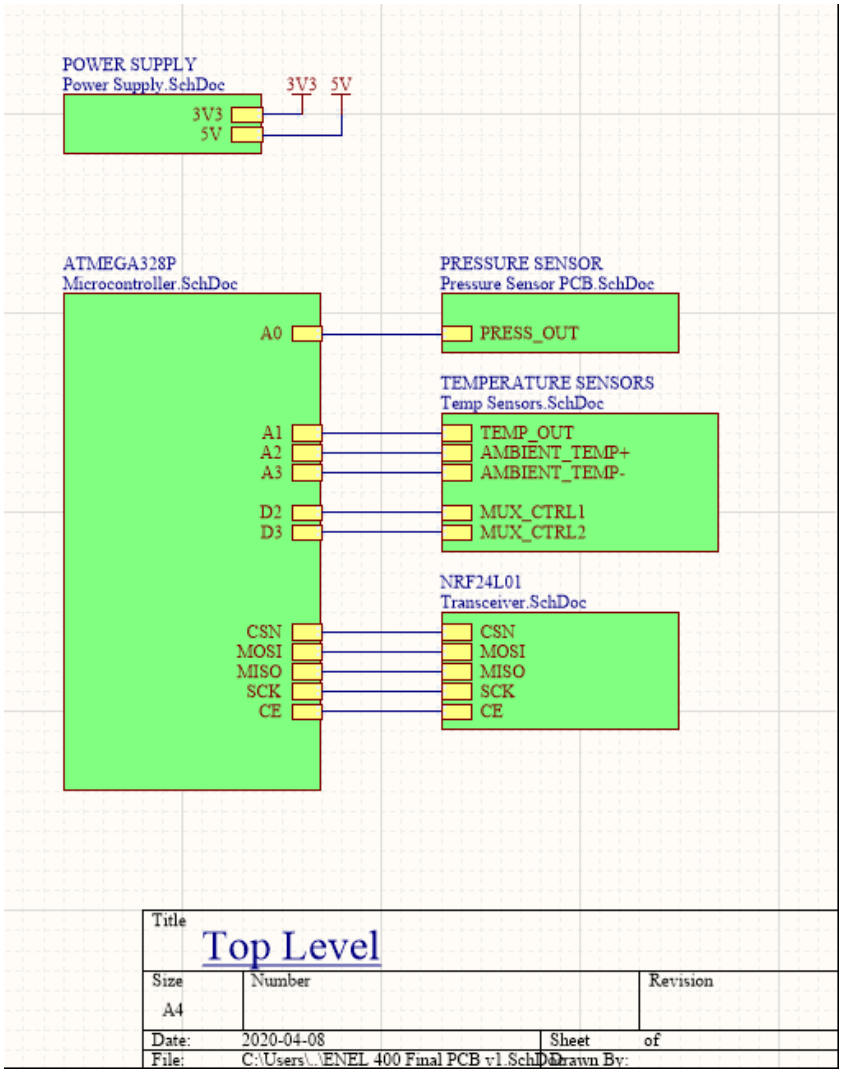

Figure 25: Top Level Schematic for Final System PCB

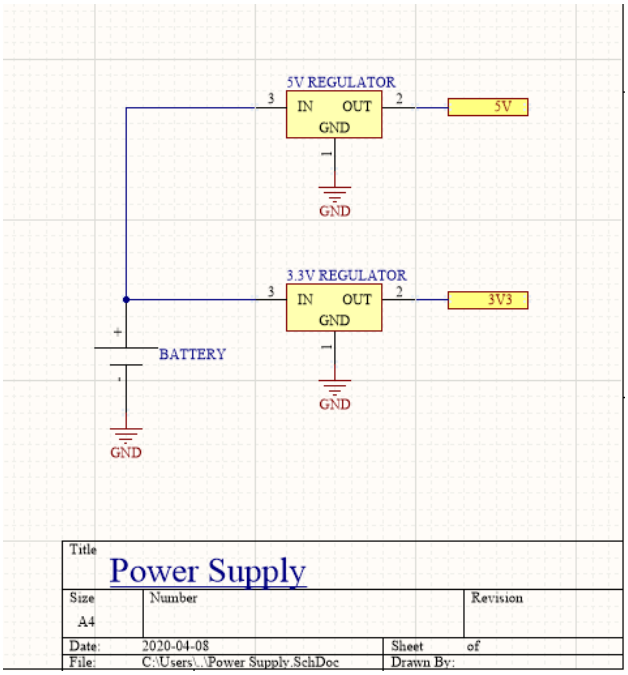

Figure 26: Power Supply Section Schematic for Final System PCB

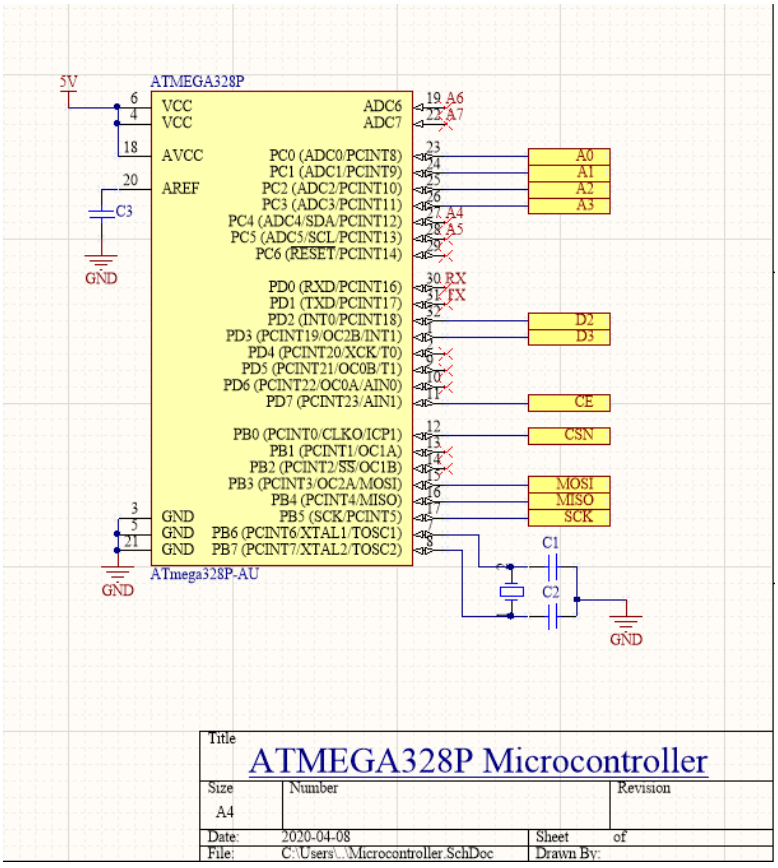

Figure 27: Microcontroller Section Schematic for Final System PCB

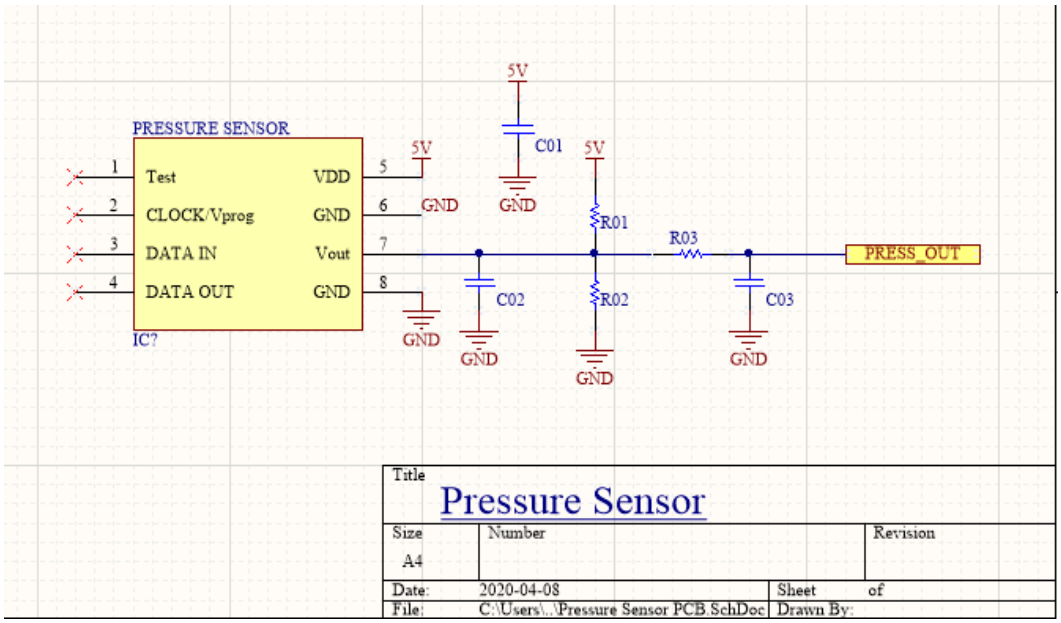

Figure 28: Pressure Sensor Section Schematic for Final System PCB

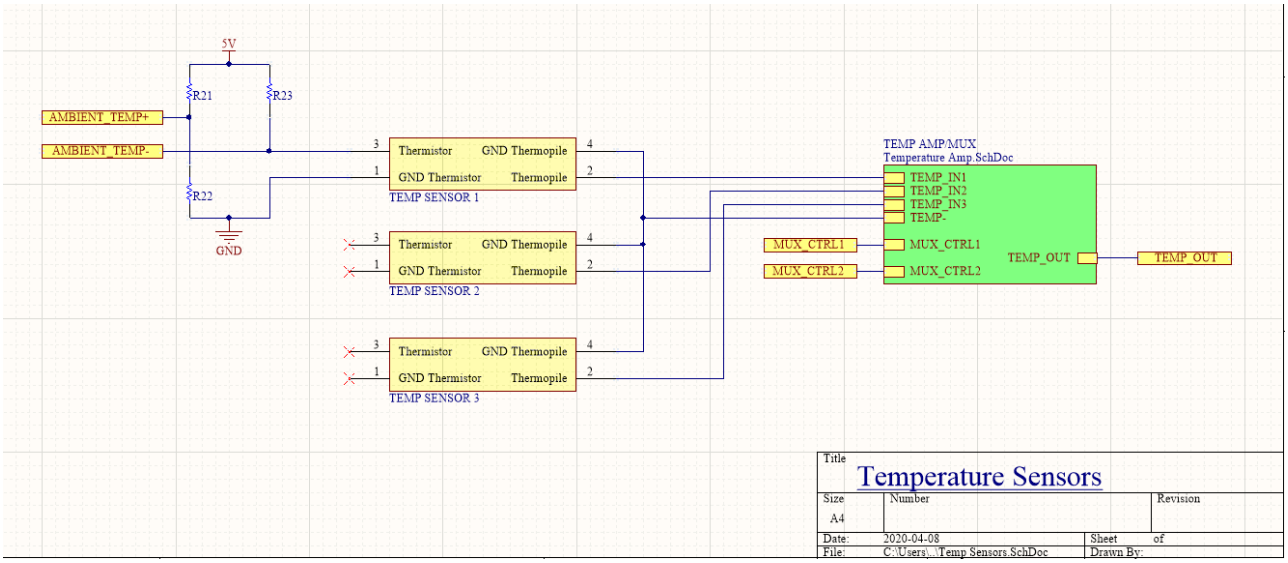

Figure 29: Temperature Sensor Section Schematic for Final System PCB

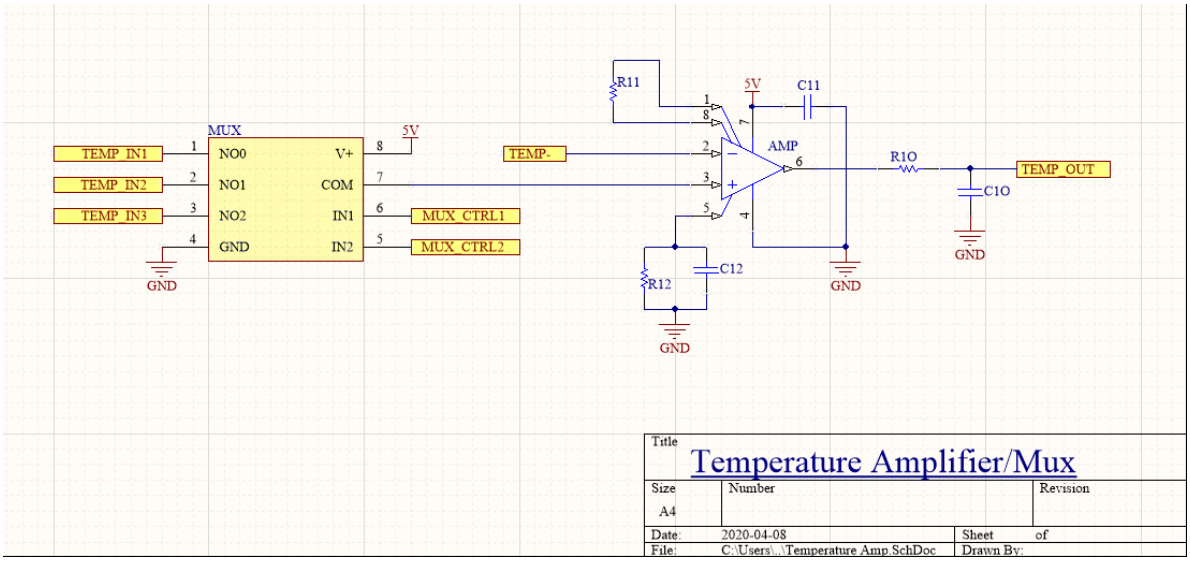

Figure 30: Temperature Amplifier/Multiplexor Subsection Schematic for Temperature Sensors in Final System PCB

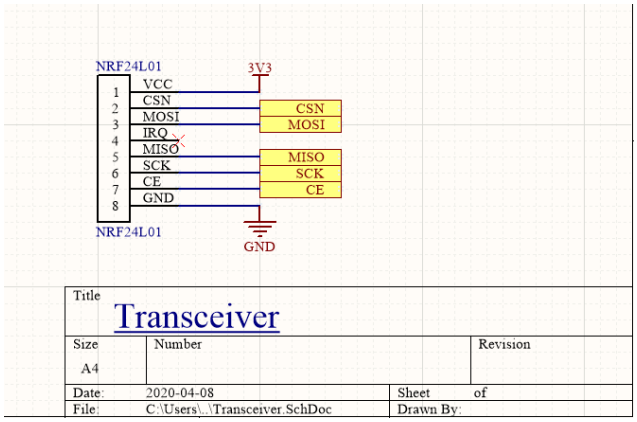

Figure 31: Transceiver Connection Section Schematic for Final System PCB

12.2 Appendix 2: PCB Layouts

12.2.1 Pressure Sensor Prototype PCB Layout

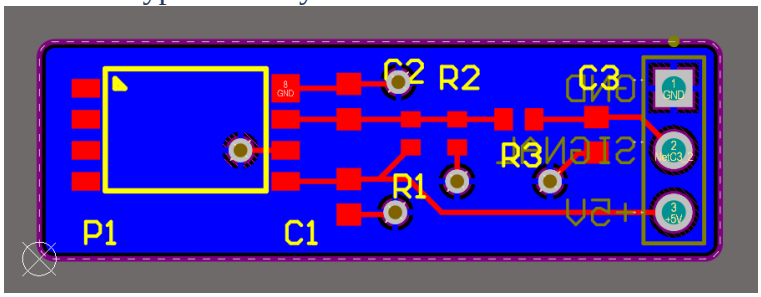

Figure 32: Pressure Sensor Prototype PCB Layout in Altium

12.2.2 Arduino Nano / NRF24L01+ Shield PCB Layout

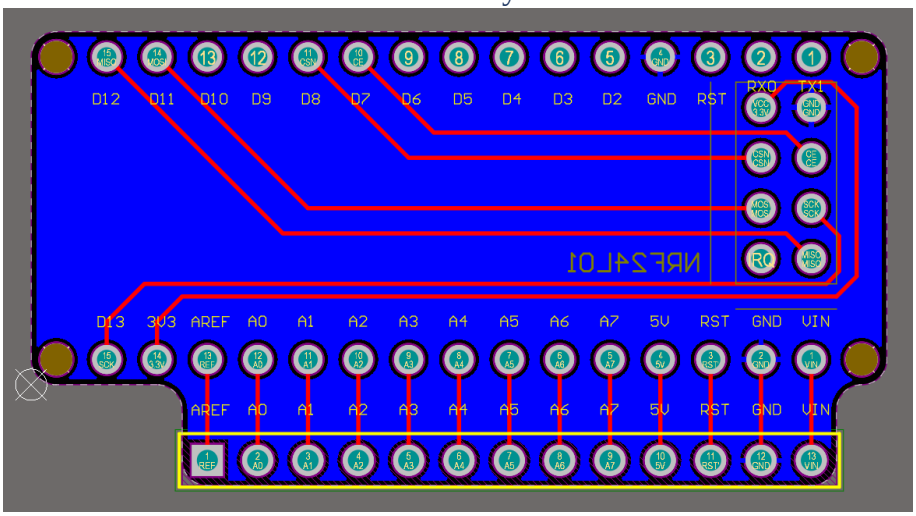

Figure 33: Arduino Nano / NRF24L01+ Shield PCB Layout in Altium

12.2.3 Final System PCB Layout

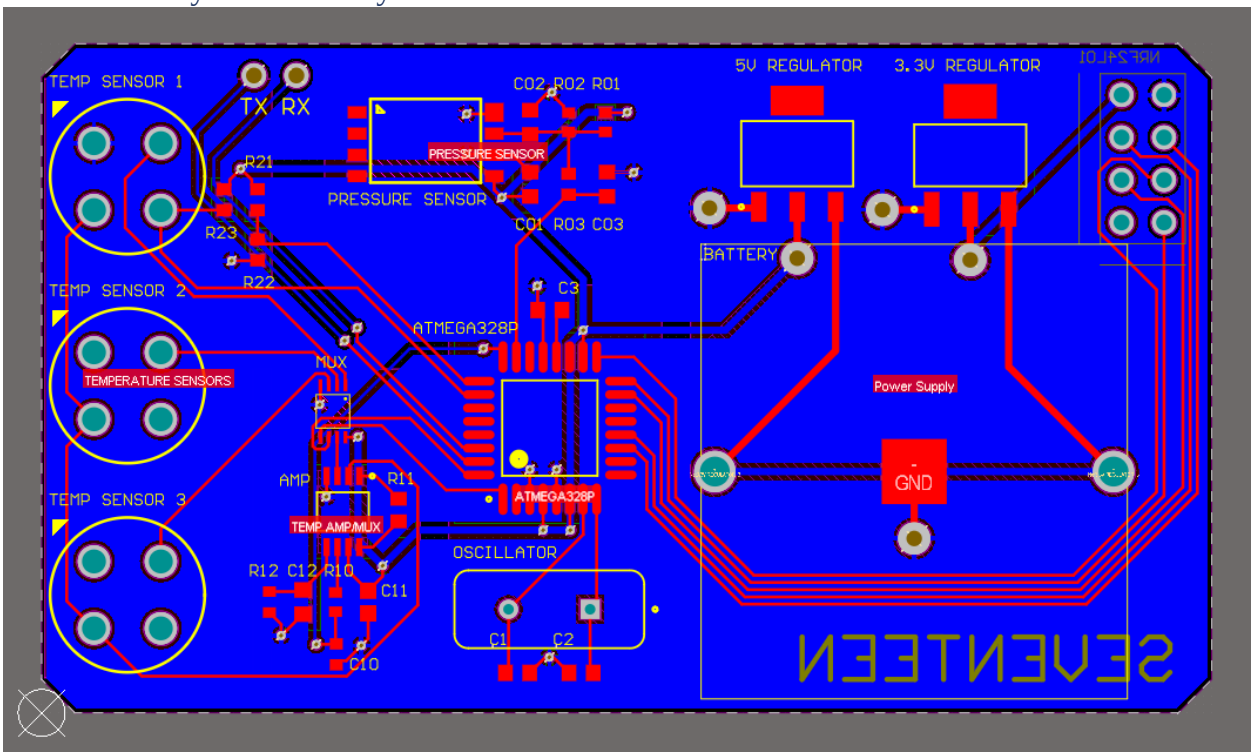

Figure 34: Final System PCB Layout in Altium

12.3 Appendix 3: Bill of Materials

12.3.1 Pressure Sensor Prototype PCB Bill of Materials

Table 12.3.1: BOM for Pressure Sensor Prototype PCB

Pressure Sensor Prototype PCB BOM

Item	Designator	Manufacturer Part Number	Manufacturer	Source	Unit Price ($)	Quantity	Total Price
Pressure Sensor	PRESSURE SENSOR	KP235XTMA1	Infineon Technologies	Mouser	$7.34	1	$7.34
0.1 uF Capacitor	C1, C2	C0603C104Z3VACTU	KEMET	Mouser	$0.14	2	$0.28
59k Resistor	R1, R2	CRCW060359K0FKEA	Vishay Dale	Mouser	$0.14	2	$0.28
22k Resistor	R3	RCS060322K0FKEA	Vishay Dale	Mouser	$0.23	1	$0.23
PCB	N/A	N/A	JLCPCB	N/A	$5.52	1	$5.52
						Total Cost:	**$13.66**

12.3.2 Final System PCB Bill of Materials

Table 12.3.2: BOM for Final System PCB

Final In-Tire System PCB BOM

Item	Designator	Manufacturer Part Number	Manufacturer	Source	Unit Price ($)	Quantity	Total Price
3.3V Linear Regulator	3.3V REGULATOR	ADP3339AKCZ-3.3-R7	Analog Devices	Digi-Key	$4.19	1	$4.19
5V Linear Regulator	5V REGULATOR	ADP3339AKCZ-5-R7	Analog Devices	Digi-Key	$4.19	1	$4.19
Op Amp	AMP	INA326EA/250	Texas Instruments	Digi-Key	$5.23	1	$5.23
Atmega Microcontroller	ATMEGA328P	ATmega328P-AU	Microchip Technology	Digi-Key	$2.01	1	$2.01
Pressure Sensor	PRESSURE SENSOR	KP235XTMA1	Infineon Technologies	Digi-Key	$7.32	1	$7.32
Temperature Sensor	TEMP SENSOR 1, TEMP SENSOR 2, TEMP SENSOR 3	ZTP-315	Amphenol Advanced Sensors	Mouser	$6.15	3	$18.45
Battery Mount	BATTERY	3025	Keystone Electronics	Digi-Key	$1.30	1	$1.30
Multiplexor	MUX	TS5A3357DCUR	Texas Instruments	Digi-Key	$0.95	1	$0.95
Oscillator	OSCILLATOR	FC4STCBMF16.0-BAG200	Fox Electronics	Digi-Key	$0.35	1	$0.35
NRF24L01+ Transceiver	NRF24L01	NRF24L01+	kuman	Amazon	$17.99	1	$17.99
22 pF Capacitor	C1, C2	GRM1885C1H220JA01D	Murata Electronics	Digi-Key	$0.12	2	$0.24
0.1 uF Capacitor	C3, C01, C02, C03, C11	C0603C104Z3VACTU	KEMET	Digi-Key	$0.10	5	$0.50
1 uF Capacitor	C1O	CL10A105KP8NNNC	Samsung Electro-Mechanics	Digi-Key	$0.10	1	$0.10
200 pF Capacitor	C12	CC0603JRNPO9BN201	Yageo	Digi-Key	$0.14	1	$0.14
59k Resistor	R01, R02	CRCW060359K0FKEA	Vishay Dale	Digi-Key	$0.10	2	$0.20
22k Resistor	R03	CRCW060322K0FKEAC	Vishay Dale	Digi-Key	$0.10	1	$0.10
100r Resistor	R1O	CRCW0603100RFKEA	Vishay Dale	Digi-Key	$0.10	1	$0.10
2k Resistor	R11	CRCW06032K00FKEAC	Vishay Dale	Digi-Key	$0.10	1	$0.10
499k Resistor	R12, R21, R22, R23	CRCW0603499KFKEA	Vishay Dale	Digi-Key	$0.10	4	$0.40
PCB	N/A	N/A	JLCPCB	N/A	$5.52	1	$5.52
						Total Cost:	**$69.38**

12.4 Appendix 4: Pictures of MVP

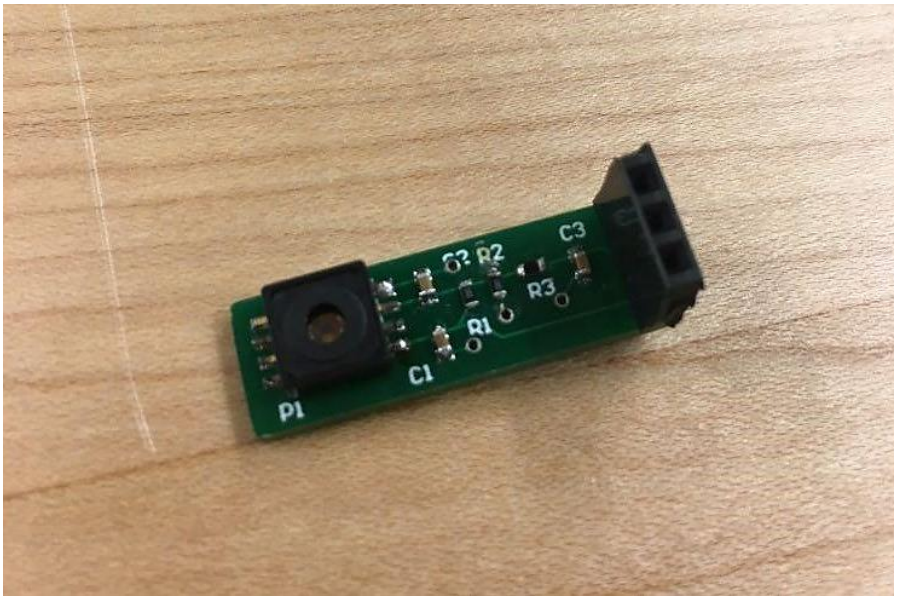

Figure 35: MVP Populated Pressure Sensor PCB

Figure 36: MVP Receiver and Microcontroller Setup

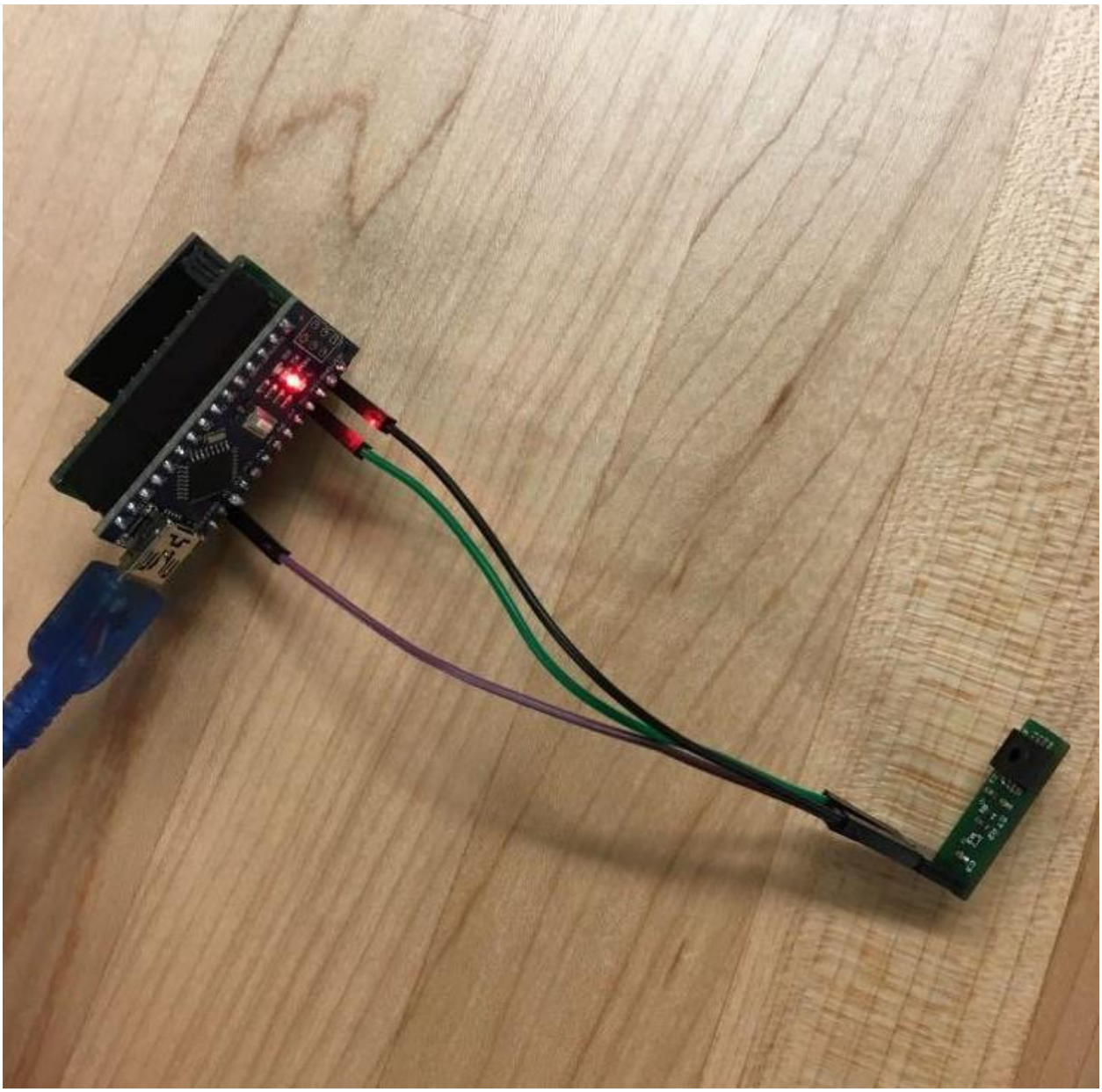

Figure 37: MVP Pressure Sensor PCB connected with the Arduino nano and the Shield PCB attaching the NRF24L01 Transceiver.

12.5 Appendix 5: 3D Model Drawings

Bottom of MVP Enclosure:

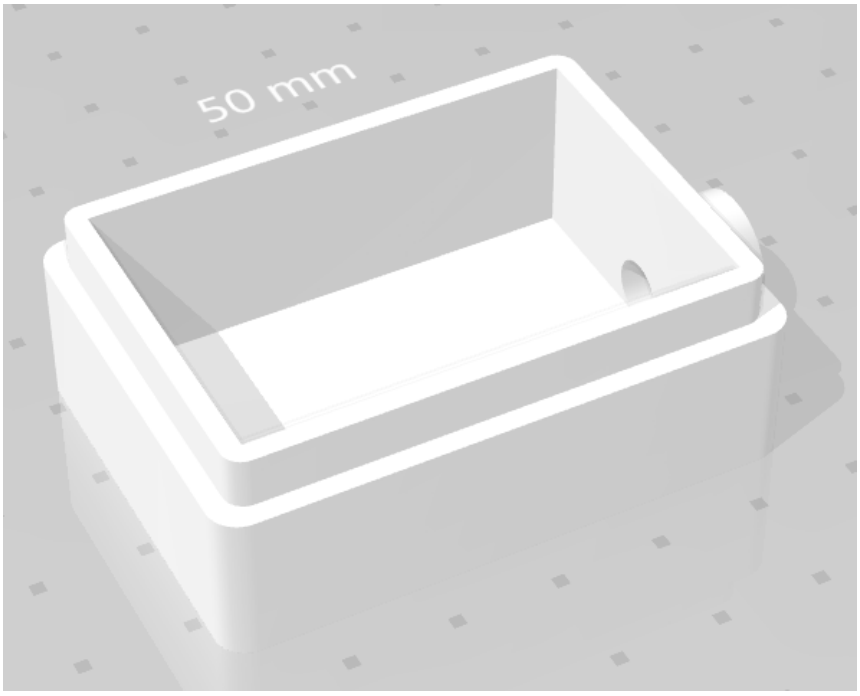

Figure 38: Bottom of MVP Enclosure

Top of MVP Enclosure:

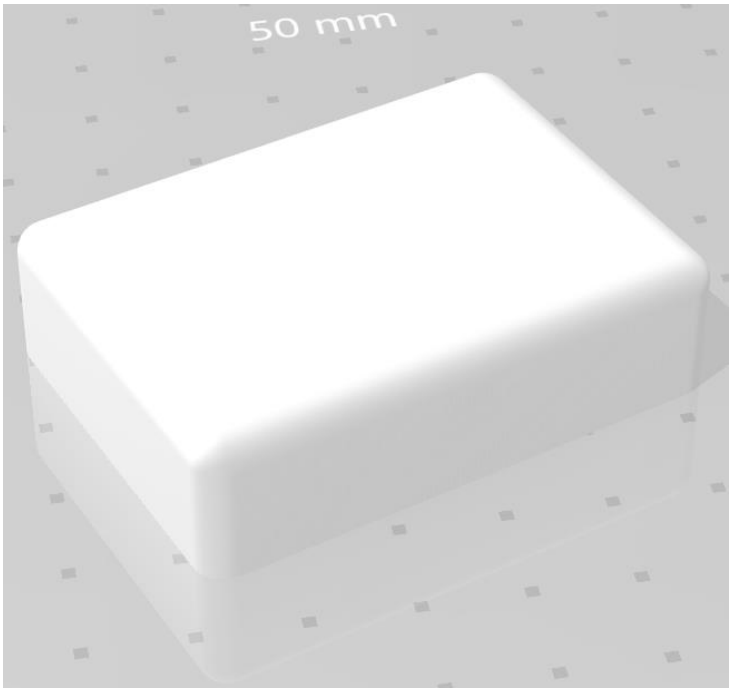

Figure 39: Top of MVP Enclosure

12.6 Appendix 6: Schedule and Expenditure Variances

To ensure team members were held accountable and the project was finished in a timely manner, a WBS was used as the initial planning tool. The WBS was used to decompose the work into required deliverables. WBS can be found below in Figure 38. After all deliverables from the WBS were identified, the team worked together to estimated required budget and duration for

each deliverable. Once all deliverables had estimates completed, the Project Manager assigned a team member responsible for each deliverable and developed a Gantt chart. The Gantt chart helped to estimate the overall duration of the project and to identify the critical path. After the critical path was identified, the slack (float) times for each task were analyzed to identify potential buffer time if the project was at risk of being delayed. The Gantt chart is depicted below in Figure 39.

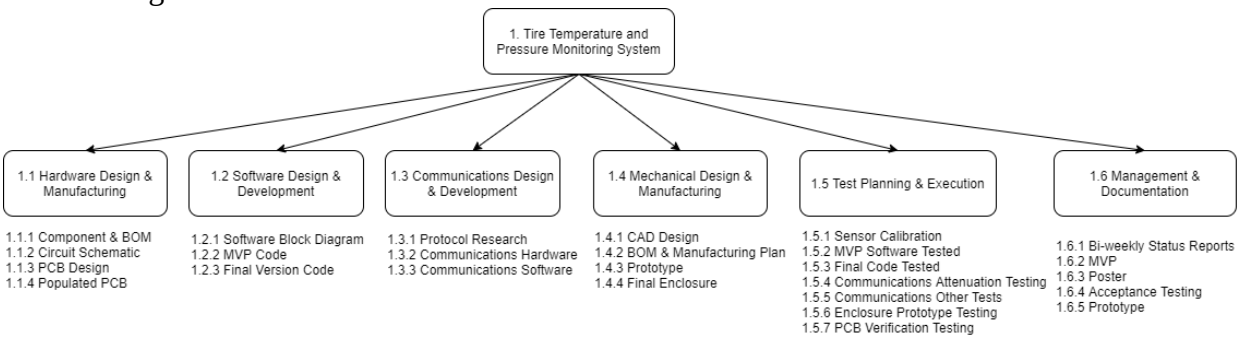

Figure 40: TTMPS Work Breakdown Structure

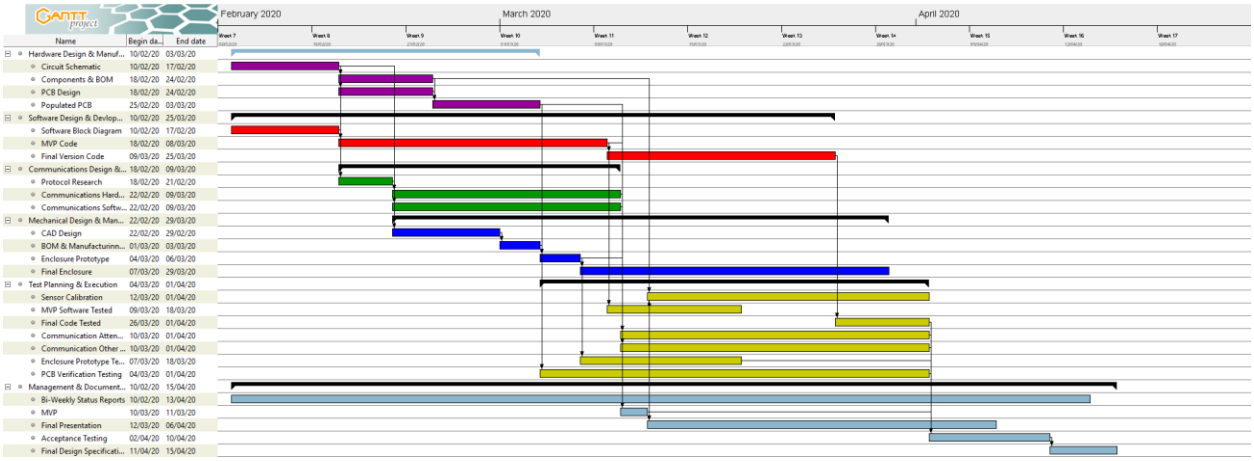

Figure 41: Gantt Chart for Team Seventeen TTPMS Project

Due to the circumstances surrounding the COVID-19 pandemic, the project was never completed as intended. However, after a team meeting when we received notice the course requirements would change, the team worked together to develop a timeline for the necessary components that were due. Due to weekly team meetings, strict deadlines, and committed team members team Seventeen did not experience any schedule variances and the project has been on schedule.

The budget for our TTPMS was set at $300, and before the change in course requirements, the total amount spent was $203.22. Outstanding items that still would have needed to be purchased included the 3:1 multiplexer, the power supply module (batteries, regulators, and other hardware), and the final PCB. The team managed the budget by working together to estimate costs of completing each deliverable in the WBS and ensuring that before any item was purchased the entire team agreed to the expense. These strategies ensured budget planning was as accurate as possible and prevented budget overages. Team Seventeen was confident that the final prototype for the TTPMS would have come in under budget. It is important to note that

while the team spent a total of $203.22 developing the prototype, the total cost listed on the BOM is only $69.38. This discrepancy arises from parts that were used in development and testing but would not be required for the final product.